Variations in esker morphology and internal architecture record time-transgressive deposition during ice margin retreat in Northern Ireland

Published in:
Proceedings of the Geologists' Association

Document Version:
Peer reviewed version

Queen's University Belfast - Research Portal:
Link to publication record in Queen's University Belfast Research Portal

1 **Variations in esker morphology and internal architecture record time-**
2 **transgressive deposition during ice margin retreat in Northern Ireland**

3 Ben J. Stoker[1,2,*], Stephen J. Livingstone[1], Iestyn D. Barr[3], Alastair Ruffell[4], Robert D. Storrar[5],
4 Sam Roberson[6]

5 [*]Corresponding author

6 [1] Department of Geography, University of Sheffield, UK, South Yorkshire, Sheffield, Winter Street,
7 S10 2TN

8 [2] Department of Physical Geography and Geoecology, Charles University, Prague, Czechia

9 [3] School of Science and the Environment, Manchester Metropolitan University, UK, Manchester,
10 Oxford Road, M15 6BH

11 [4] School of Natural and Built Environment, Queens University Belfast, UK, Belfast, Elmwood Avenue,
12 BT7 1NN

13 [5] Department of the Natural and Built Environment, Sheffield Hallam University, UK, Sheffield,
14 Howard Street, S1 1WB

15 [6] Geological Survey of Northern Ireland, Dundonald House, Belfast, BT4 3SB, UK

16 Keywords: Eskers, Northern Ireland, morphology, sedimentology, deglaciation, meltwater

17 **Abstract**

18 The architecture and evolution of the subglacial hydrological system plays a key role in modulating
19 ice flow. Eskers provide an opportunity to understand subglacial hydrology at a broader temporal and
20 spatial perspective than contemporary studies. Recent research has established a morphogenetic
21 classification for eskers, but these studies have been limited to topographically simple regions of a
22 single ice sheet. We present an updated map of esker distribution in Northern Ireland based on 5 m
23 resolution elevation data, and a high-resolution map (0.4 m resolution) of the glacial geology of SW
24 Northern Ireland. Ground Penetrating Radar data from four sites along the >20 km long Evishanoran
25 esker system in central Northern Ireland are combined with geomorphological observations to provide
26 an insight into depositional processes and controls on esker formation. Esker architecture indicates
27 two main phases of formation, including an initial stage of high energy flow in a subglacial conduit
28 followed by a final stage of waning flow energy closer to the ice sheet margin. These waning flow
29 energy deposits can be used to reconstruct the ice margin retreat rate and pattern. We identify that
30 local topographic complexity and geological conditions (e.g. fault control) are important controls on
31 subglacial hydrological processes. The broad-scale esker architecture remains the same despite
32 variable esker morphology (planform), while there are significant variations in local topography and

geology. We suggest that this represents local factors controlling esker morphology, as hydrological processes alone cannot explain these variations. This study provides further evidence that morphogenetic relationships cannot be based solely on remote sensing data and must be supported by robust field data, especially where post-glacial processes may distort esker morphology (e.g. peat infilling).

1.0 Introduction

The distribution of meltwater at the base of ice sheets influences ice motion by modulating basal sliding and deformation of sediments. The influence of water on ice flow depends on the architecture of the subglacial drainage network and how it evolves to accommodate water inputs (e.g. Budd et al., 1979; Alley et al., 1986; Iken and Bindshadler, 1986). Efficient low-pressure networks of discrete channels rapidly drain water to the margin and tend to reduce ice velocity (Hubbard and Nienow, 1997). Inefficient distributed networks (e.g. linked cavities, canals and a porous till layer) result in increased effective pressure, in turn leading to higher ice velocities (Röthlisberger, 1972; Schoof, 2010). Recent observations from beneath the Antarctic and Greenland ice sheets have implicated dynamic subglacial water systems in driving rapid ice-flow variations (Zwally et al., 2002; Bell et al., 2007; Stearns et al., 2008; Bartholomew et al., 2010; Davison et al., 2019).

For investigations of subglacial hydrological processes, the imprint of meltwater drainage, recorded on the beds of former ice sheets, has a clear advantage over data from contemporary ice sheets (e.g. borehole surveys) because it is possible to reconstruct the history of meltwater drainage over centennial to millennial time-scales and spatially over metres to hundreds of kilometres. These temporal and spatial scales not only allow a more complete understanding of the architecture and evolution of the subglacial drainage network but are relevant for informing numerical modelling experiments (cf. Greenwood et al., 2016; Hewitt & Creyts, 2019). Eskers are the depositional imprint of drainage through subglacial (R-channels), englacial or supraglacial channels (Price, 1969; Banerjee and McDonald, 1975; Gustavson and Boothroyd, 1987; Brennand, 2000) and are commonly found across the beds of former ice sheets (e.g. Storrar et al., 2014a; Stroeven et al., 2016; Clark et al., 2018). They typically comprise elongate ridges of fluvioglacially deposited sand and gravel that can extend tens to hundreds of kilometres, are arranged roughly parallel to former ice flow direction, and range from single ridges to more complex anabranching forms (e.g. Flint, 1930; Brennand, 1994; Burke et al., 2012; Storrar et al., 2015; Perkins et al., 2016). Esker geometry, distribution and sedimentary architecture have been widely used to reconstruct drainage pathways and infer past ice sheet dimensions and dynamics (e.g. Shreve, 1985; Dyke and Prest, 1987; Aylsworth and Shilts, 1989; Hebrand and Åmark, 1989; Clark and Walder, 1994; Brennand, 1994, 2000; Warren and Ashley, 1994; Margold et al., 2013; Storrar et al., 2013, 2014a; Livingstone et al., 2015). However, there is still considerable uncertainty over the genesis of eskers, including the extent to which they form time-transgressively or synchronously (e.g. Brennand,

68 2000; Makinen, 2003; Cummings et al., 2011); the magnitude and frequency of drainage (Burke et al.,

69 2008, 2010, 2012; Livingstone et al., 2016; Drews et al., 2017); and the vertical position in the ice mass

70 (i.e. supraglacial, englacial or subglacial) in which they are deposited (Price, 1969; Fitzsimmons, 1991;

71 Perkins et al., 2016).

72 Understanding how eskers form is important for reconstructing palaeo-ice sheets and providing

73 information on subglacial hydrological processes. In particular, the varied form and architecture of

74 eskers is thought to be controlled by the hydrological properties of the channelised drainage system

75 (Burke et al., 2015; Storrar et al., 2015). For example, recent morpho-sedimentary studies of eskers in

76 southern Alberta, Canada, and mapping of eskers emerging from the front of Breiðamerkurjökull,

77 southeast Iceland, have related abundant meltwater and sediment supply to complex esker systems, and

78 low sediment supply and either high or low meltwater abundance to single ridges of uniform geometry

79 (Burke et al., 2015; Storrar et al., 2015, 2020). A barrier to understanding the formation of eskers at the

80 ice sheet-scale is the relative dearth of sedimentological investigations of these long esker systems.

81 Recent work (e.g. Burke et al., 2012; Perkins et al., 2013) has begun to address this using geophysical

82 investigations of the sedimentary architecture of eskers formed beneath the Cordilleran Ice Sheet. To

83 further investigate the relationship between ice sheet hydrology and esker properties, this paper

84 combines detailed geomorphological, geophysical and sedimentological data to assess controls on the

85 formation of a ~20 km long esker network in Northern Ireland (UK) whose morphology changes down-

86 flow from a complex multi-ridge system to a large single ridge.

87 **2.0 Background**

88 *2.1 Glacial history of Ireland*

89 The early stages of the onset of the Irish Ice Sheet (~ 35 ka) were characterised by incursion of Scottish

90 ice flowing in from the NE, which subsumed localised ice caps over Irish upland massifs (Colhoun,

91 1971; Clark and Meehan, 2001; Greenwood and Clark, 2009b). As Irish ice coalesced with western

92 Scottish ice, the location of the dominant ice dispersal centres migrated to upland areas in the west of

93 Ireland, exerting a strong control on ice flows patterns (Greenwood and Clark, 2009b). Heterogenous

94 growth patterns led to ice sheet sectors reaching their maxima at different times. For example, the

95 western margin reached its maximum position relatively early compared to the southern portion of the

96 ice sheet (Ó Cofaigh and Evans, 2007; Greenwood and Clark, 2009b; Ó Cofaigh et al., 2019). The

97 configuration of ice domes and the geomorphology of the Irish Ice Sheet required ice expansion onto

98 the continental shelf, with the Last Glacial Maximum (LGM; 23 ka – 18 ka) resulting in almost complete

99 terrestrial ice coverage across Ireland (Knight et al., 2004; Ó Cofaigh and Evans, 2007; Bradwell et al.,

100 2008; Greenwood and Clark, 2009a,b; Clark et al. 2018).

Deglaciation in Ireland was characterised by the migration of competing ice divides, which resulted in a complex deglacial history (Knight, 2003, 2019; Greenwood, 2009b). The ice sheet fragmented as it retreated into upland dispersal centres such as the Connemara Mountains in Western Ireland and County Donegal to the north (Wilson *et al.,* 2019), or lowland ice domes situated in the Lough Neagh Basin and Omagh Basin (Fig. 1). Ice sheet retreat is thought to have been interspersed with asynchronous phases of localised ice advance or stagnation, likely related to the migration of ice divides (Knight, 1999; Knight, 2006; Clark *et al.,* 2012; Chiverrell *et al.,* 2020). Within central Northern Ireland, the two dominant LGM ice dispersal centres were situated in the Lough Neagh basin, and in the Sperrin Mountain range to the north (Fig. 1) (Knight, 1999). During this period, SW ice flow dominated from an ice dome in the NE Omagh Basin offshore towards the Donegal Bay (Fig. 1), indicated by an area of subglacial ribs across the Omagh Basin (Knight and McCabe, 1997). Subglacial ribs across central Northern Ireland often display modification or drumlinisation likely associated with changes in ice flow patterns and subglacial thermal regime (Knight, 1997; Knight and McCabe, 1997). An ice flow reversal occurred during deglaciation when the dominant ice dome over the Omagh Basin migrated SW to the Lower Lough Erne basin, leading to NE ice flow forming a prominent esker system overlying the subglacial ribs (Knight, 2004). The regional retreat pattern to the SW is documented by a series of meltwater landforms, including eskers. The final stages of deglaciation were characterised by localised mountain ice caps, with the last remnants of the Irish Ice Sheet likely located in the mountains of Donegal in the northwest (Greenwood and Clark, 2009b; Smith and Knight, 2011).

Research into the meltwater systems of Ireland has a long history stretching back to the late 19th century, and has concentrated on the origin of the large (up to 50 m high) ridges of the Esker Riada system in the Irish Midlands (Sollas, 1896; Gregory, 1912, 1921; Hinch, 1921; Flint, 1930). Theories on the origin of these eskers revolved around whether they were deposited by a sub- or supraglacial river system, or whether they represented deltaic fluvioglacial deposits (Gregory, 1921). More recently, studies have debated whether the Esker Riada system and associated fluvioglacial sediments were deposited by meltwater in an interlobate position, between two retreating ice masses (Warren and Ashley, 1994; Pellicer et al., 2012), or as part of a multi-phase model involving westerly ice sheet retreat, followed by a period of ice sheet readvance from the north (Delaney, 2001a, b, 2002; Delaney et al., 2018). The eskers of central Northern Ireland have been used to reconstruct the migration of ice domes and time-transgressive variations in the subglacial drainage system (Knight, 1997; 2019), but historically, there has been less research focused on them.

2.2 Regional Context and Landform Distribution

Central Northern Ireland incorporates the Sperrin Mountains to the north and the Omagh Basin; a low elevation region of undulating topography, to the south (Fig. 1). The regional geology is varied, with a series of folded and faulted Palaeozoic sandstones and limestones to the south, and crystalline granites

136 and gabbros to the north (Knight, 1997; Geological Survey Northern Ireland, 2016). A series of three

137 large, subparallel fault lines trend NE-SW and define geological boundaries, while smaller faults with

138 a variety of orientations are also prevalent (Geological Survey Northern Ireland, 2016).

139 A range of glacial landforms have been documented across the region, including meltwater channels,

140 eskers, drumlins and subglacial ribs (Colhoun, 1970; Knight, 2003; Clark et al., 2018). Major moraines

141 are largely absent across central Northern Ireland, being restricted to the present coastline and the

142 continental shelf onto which the Irish Ice Sheet extended (Clark et al., 2018). An area of subglacial ribs

143 dominates the lowland areas across Central Northern Ireland, with ridge crestlines oriented

144 perpendicular to SW ice flow during the LGM (Knight and McCabe, 1997; Knight, 2003). These

145 subglacial ribs are commonly drumlinised or exhibit modification by meltwater, which may have been

146 stored in the lowland area between ridge crestlines (Knight and McCabe, 1997; Knight, 2003, 2006).

147 Alongside subglacial ribs, E-W orientated drumlins dominate the lowlands of the Omagh and Lough

148 Erne Basins (Knight, 1997, 2003). A prominent esker system located in the NE of the Lower Lough

149 Erne Basin forms a series of bifurcating ridges in a meltwater valley dissecting the zone of subglacial

150 ribs (Fig. 2a). This system was deposited under NE ice flow during deglaciation to the SW, contrasting

151 with the SW ice flow responsible for the formation of the subglacial ribs. Therefore, these eskers

152 represent a reversal of the hydraulic gradient as the ice dome situated over the Omagh Basin migrated

153 towards the Lower Lough Erne Basin (Knight and McCabe, 1997).

154 The present study focuses on a >20 km long complex esker system in County Tyrone, Central

155 Northern Ireland. The esker complex trends out of three meltwater channels cutting through the

156 hills to the south, and terminates near the Davagh Forest in the north (Figs. 2 and 3). The NE sector

157 was mapped in part by Gregory (1925) and termed the Evishanoran Esker. Early debate sought to

158 identify whether deposition was associated with local ice masses from the east, or related to a larger

159 ice mass from the southwest (Charlesworth, 1926; Gregory, 1926). Here we refer to the entire esker

160 complex as the Evishanoran Esker, including newly mapped segments that were not documented

161 in Gregory (1925).

162 **3.0 Methods**

163 *3.1 Geomorphological mapping*

164 Comprehensive mapping of esker ridges was undertaken for the whole of Northern Ireland. Landform

165 mapping was performed within ArcGIS 10.4.1, using a 5 m resolution digital elevation model (DEM)

166 produced by the Land and Property Services Northern Ireland under MOU205, provided to Queens

167 University Belfast. We also mapped all glacial landforms across the study area of SW Northern Ireland

168 using a ~0.4 m resolution digital surface model (DSM) to provide geomorphological context of the area

169 surrounding the Evishanoran Esker (Fig. 2).

170   Landform identification was based on morphology, association with other features and local
171   topography. Landforms were digitized as either polylines or polygons. Esker crestlines were digitized
172   as polylines to investigate broad-scale distribution and morphological characteristics. Fan-shaped
173   enlargements located at esker termini were classified as esker fans and digitized as polygons at the break
174   of slope. The thalwegs of meltwater channels were digitized as polylines and classified as either
175   subglacial or lateral according to the criteria set out by Greenwood *et al* (2007). All subglacial bedforms
176   were mapped as polygons, including: subglacial ribs (ribbed moraine), drumlins, mega-scale glacial
177   lineations, and streamlined bedrock features. Our mapping builds on earlier low-resolution mapping
178   from Landsat and SPOT satellite imagery and field surveys (Knight, 2003; Greenwood and Clark,
179   2009a), and has resulted in the creation of a comprehensive database of Northern Irish eskers, consistent
180   with the NextMap 5 m resolution data used for the rest of the UK (Clark et al., 2018), and detailed
181   mapping of glacial landforms in SW Northern Ireland at 0.4 m resolution.
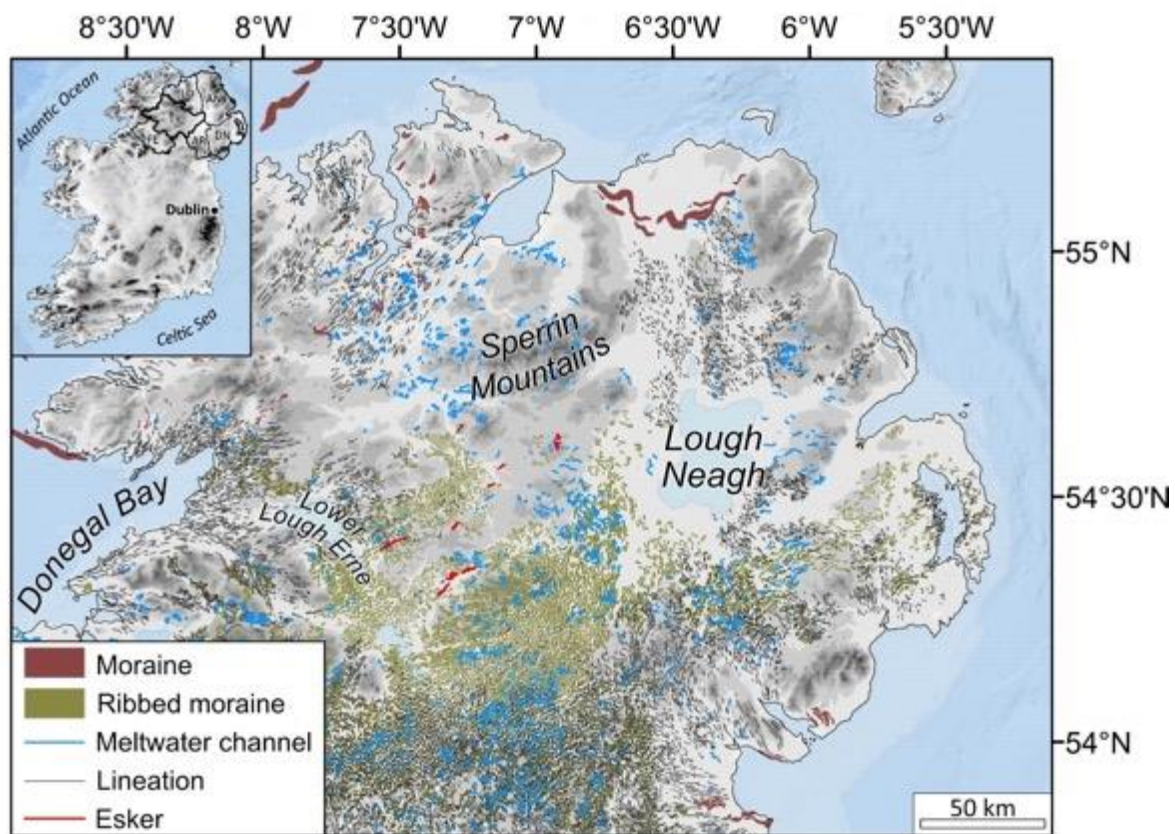
183   Figure 1. The distribution of mapped glacial landforms within the BRITICE v2 database across
184   Northern Ireland (Clark *et al.,* 2018). Subglacial lineations include Mega-Scale Glacial Lineations and
185   drumlins.

186   *3.2 Ground Penetrating Radar*

187   Ground Penetrating Radar (GPR) data were acquired in August and November 2016. A total of ~1.8
188   km are presented here, including profiles along the crestlines of the eskers and cross profiles in a range

189 of topographic contexts and for different esker forms. A 32-bit Mala Ground Explorer (GX) controller
190 unit connected directly to a 160MHz GX shielded antenna on a rough terrain skid plate was used in
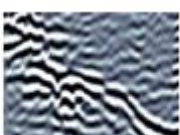191 August 2016. Radar profiles were acquired at a constant walking pace in a continuous, time-triggered
192 shot mode using hyperstacking to reduce random noise. A Mala Ramac system consisting of a 4 m-long
193 Rough Terrain Antenna, comprising in-line, unshielded transmitting and receiving antennas with a 1.5
194 m spacing and 100MHz centre frequency was used in November 2016. Collection of radar data was
195 performed at a constant walking pace, in a time-triggered mode, with 16 stacks at a delay of 0.5-seconds.
196 All radar survey lines were simultaneously mapped using a Leica CS15 differential Global Positioning
197 System (dGPS) unit to topographically correct the profiles.

198 Processing of radar data was performed within REFLEXW v7.5.9, the proprietary software of Karl
199 Sandmeier under licence number 401 provided to Queen's University, Belfast. A standard processing
200 sequence was developed, using the following steps: static correction of time-zero drift, removal of low
201 frequency signal saturation (dewow), application of gain to increase the visibility of reflections at depth,
202 diffraction stack migration, background removal to reduce antenna ringing, bandpass filtering and
203 topographic correction with the associated dGPS trace, finally radargrams were plotted in MatLab
204 v9.1.0.441655 (Neal, 2004; Cassidy and Jol, 2009). A velocity of 0.1 m/ns for migration was used,
205 consistent with exposures of eskers in sand extraction pits, hillside scars and road-cuts (see section 3.3)
206 (Russell et al., 2001; Pellicer et al., 2012; Livingstone et al., 2016). GPR profiles were interpreted by
207 identifying high-amplitude reflectors indicative of bounding surfaces between radar facies. Six radar
208 facies (*sensu* Gawthorpe *et al.,* 1993) were differentiated based upon depositional characteristics,
209 including associations with sediment facies identified from exposures in the field and the broad
210 characteristics of reflectors within a unit (Table 1). Lateral discontinuities and offset reflectors were
211 interpreted as geological faults (e.g. Fiore et al., 2002).
212
213 *3.3 Sedimentology*
214 Gravel pit exposures adjacent to, and below, the GPR profiles were investigated to provide an insight
215 into the flow conditions responsible for ridge formation in the Evishanoran Esker, and to provide
216 ground-truthing for the interpretation of radargrams. Four sediment exposures were logged within the
217 complex, multi-ridge system and the simple, single-ridge system (Fig. 2). Scaled sediment logs were
218 drawn to record stratigraphic data, including details on the sedimentary structures, texture, and the unit
219 characteristics, such as bed geometry and contacts. Lithofacies were based on Evans and Benn (2004).
220 Clast macrofabric and palaeoflow indicators (e.g. ripples) supplemented stratigraphic logs (Miall,
221 1985).

Table 1. Summary of key radar facies observed along the Evishanoran Esker, including both fluvioglacial and post-glacial features. Further description and interpretation of radar facies is presented in section 4.2.1.

Facies type	Radar facies example	Facies characteristics	Facies Interpretation
Esker ridge facies		Radar Facies 1: Chaotic, discontinuous reflectors.	Coarse gravel formed subglacially under high flow velocities (Burke et al., 2015)
		Radar Facies 2: Sub-horizontal, moderately continuous reflectors.	Vertical accretion of fine-grained material (Burke et al., 2012)
		Radar Facies 3: High-angle, downflow dipping reflections.	Fine-grained, foreset deposits (Burke et al., 2010)
		Radar Facies 4: Concave, basin-like reflectors.	Scour-and-fill basins (Perkins et al., 2016)
Post-glacial facies		Radar Facies 5: Attenuated, horizontal reflections.	Post-glacial peat infill (Jol and Smith, 1991)

226
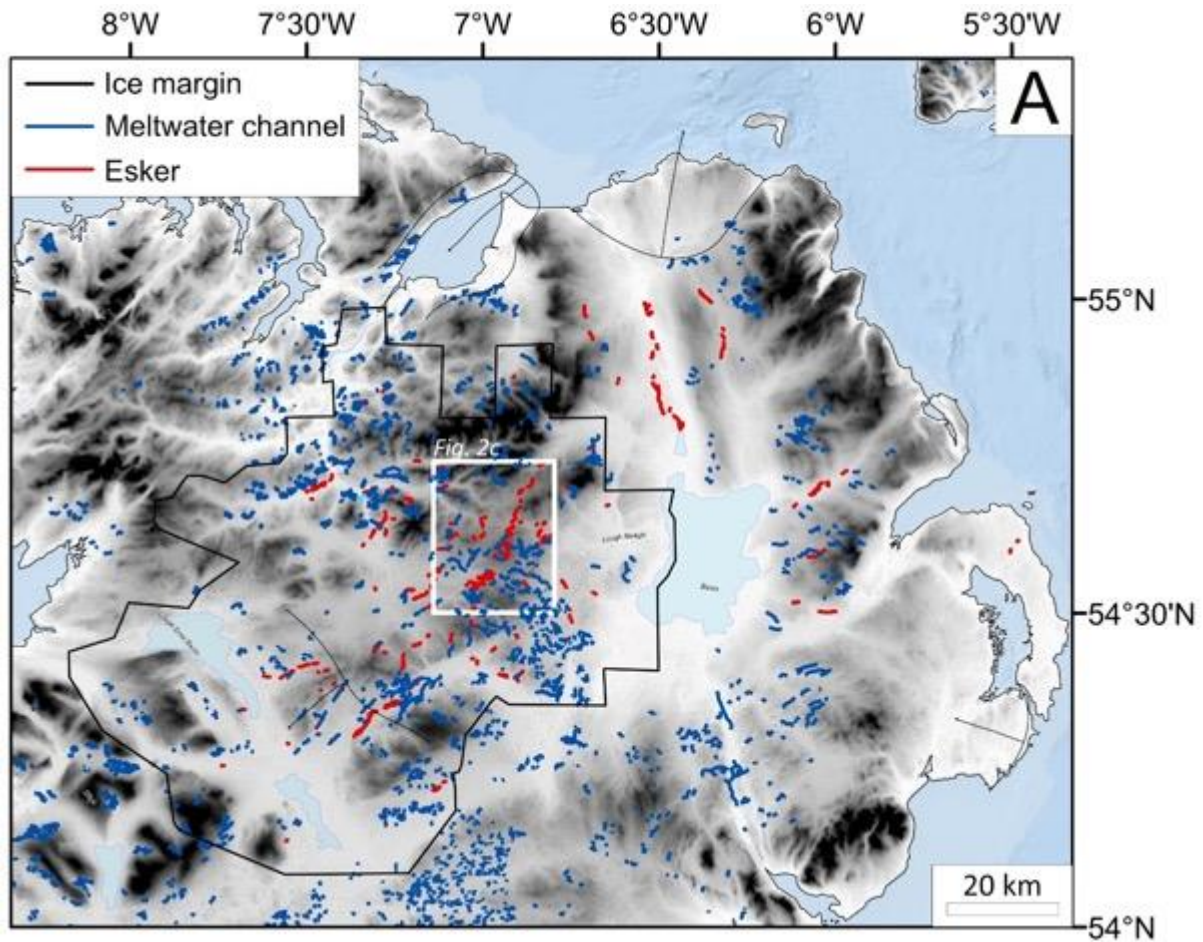
Figure 2. (a) An updated map of meltwater landforms of Northern Ireland, including features mapped

in this study. Meltwater channels from the BRITICE v2 compilation are also included (Clark *et al.,*

2018). Note the occurrence of a large esker system to the west of Lough Neagh, unreported in the

BRITICE database. Ice margin positions are adapted from Greenwood and Clark (2009b), with arrows

showing ice margin retreat direction. The black box indicates the extent of high-resolution (~0.4 m)

DSM coverage used within this study and shown in Figure 2b.

233
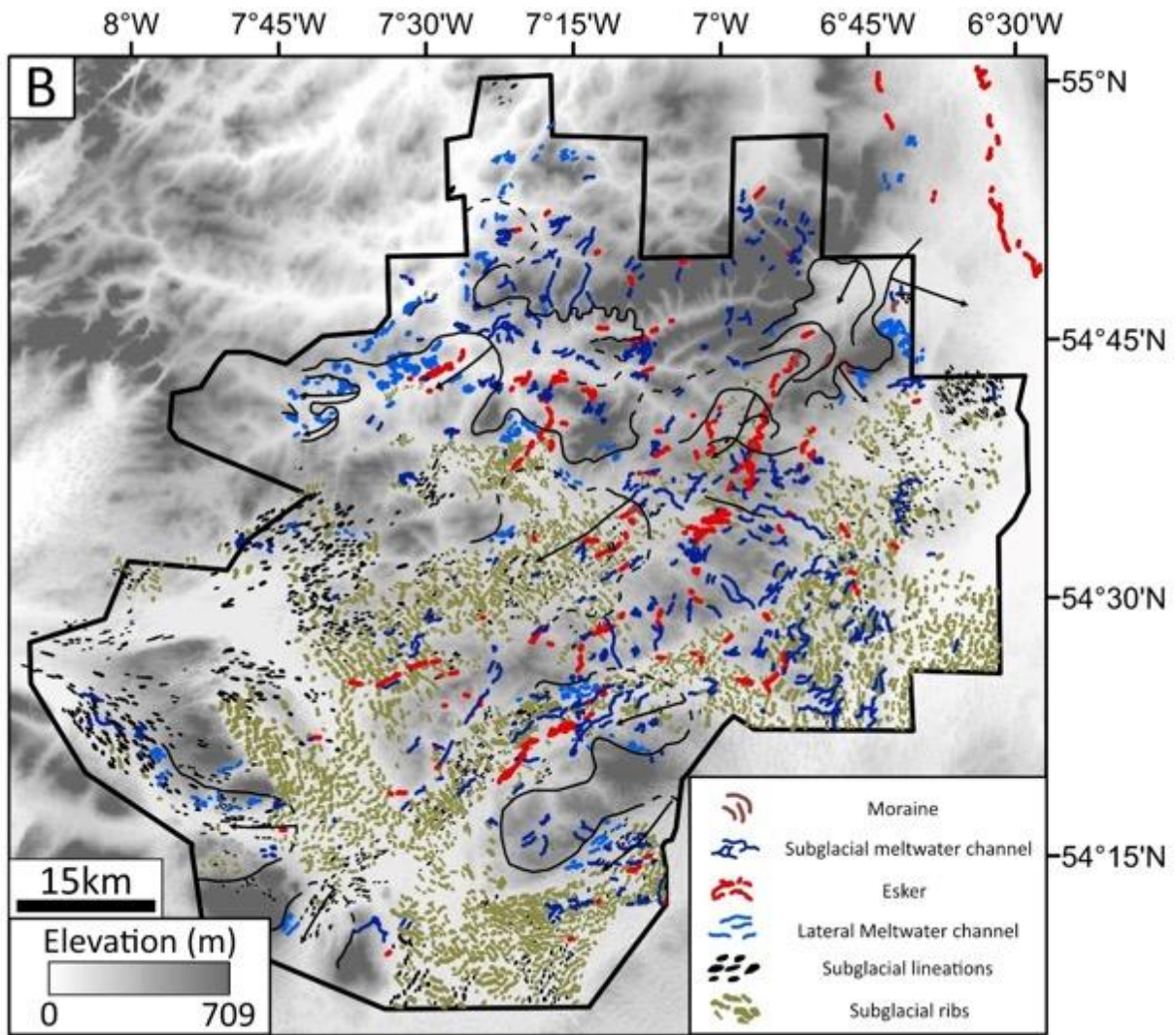
Figure 2. (b) Glacial geomorphology of SW Northern Ireland based on a 0.4m DSM. Schematic ice margin positions (black lines) have been drawn based on esker morphology, fan deposits, lateral meltwater channels and moraines. Dotted black lines indicate areas of lower certainty in ice margin position. Black arrows indicate ice margin retreat directions. The white outline indicates the extent of DSM coverage.

240
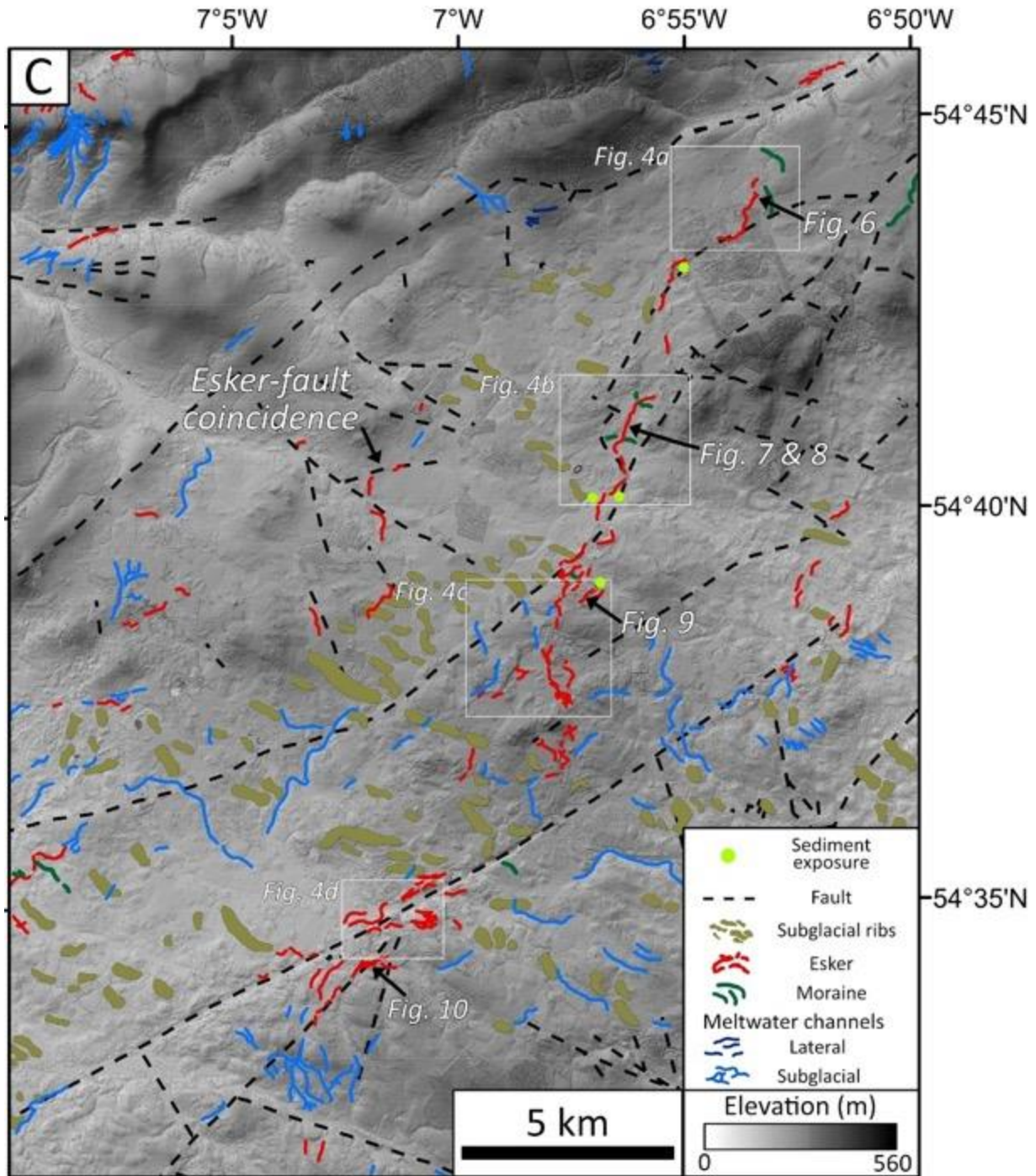
Fig. 2c. The esker system in County Tyrone, annotated with the location of investigated sediment exposures. Note the coincidence of the southern esker system with a large SW-NE trending fault, while some eskers in the northwest demonstrate dramatic changes in orientation to follow fault lines. White boxes highlight features detailed within Fig. 4. Geological faulting data is based on the 10K geology dataset, reproduced with the permission of the Geological Survey of Northern Ireland. Crown Copyright 2018.

247

4.0 Results and interpretations

4.1 Glacial Geomorphology

A complete map of the glacial meltwater landforms of Northern Ireland is presented in Fig. 2a. The map contains 457 esker ridges, totalling 219.6 km in length, compared to 63 esker ridges (39.4 km) detailed for this region in the BRITICE v2 database (Clark *et al.,* 2018). Esker distribution is heterogenous, with the majority concentrated in a NE-SW axis to the south of the Sperrin Mountains. A > 20 km long N-S trending esker system is present to the north of the Lough Neagh Basin. Meltwater channels most commonly occur near upland regions (Fig. 2a). Meltwater channels have been documented by previous mapping efforts and are ubiquitous across Northern Ireland (Charlesworth, 1924; Colhoun, 1970; Knight, 2006; Greenwood and Clark, 2009a).

We present a detailed map of the glacial geomorphology of SW Northern Ireland in Fig. 2b, including moraines, meltwater channels (lateral and subglacial), eskers and subglacial bedforms (lineations and ribs). To the south of the Sperrin Mountains, a complex system of over 80 ridges form the Evishanoran esker system, spanning > 20 km and demonstrating considerable variation in morphology over its length (Fig. 2 and 3). The esker system is oriented SW-NE, broadly aligned with an area of subglacial ribs. Across this region, further fluvioglacial landforms associated with the esker system are observed. Most notably, the SW sector is associated with a series of subglacial meltwater channels cut into a slope that trends against the regional northwards ice flow, outwash fans are located at the northern terminus of some eskers, and a kame terrace is observed on the southern slopes of the Sperrin Mountains. We define three distinct esker sections based on variations in esker planform; the northern sector of the esker is composed of a predominantly simple system of single ridges, the central sector is dominated by a complex, arborescent ridge network distributed around a hill (~100m relief), and the southern sector comprises a complex, anabranching system of multiple subparallel ridges (Figs. 3, 4).

In the northern sector of the esker system (Fig. 4a,b), a simple planform dominates, consisting of nine consecutive ridges, with a total length of ~9 km (Table 2). The esker system trends uphill towards the NE, with ridges orientated along a uniform, broad valley bottom. However, the eskers in this sector are morphologically complex. Some adjacent ridge segments display an offset relationship, while others terminate in fans at their northern end, or may exhibit enlargements in the esker profile (Fig. 4b; Table 2). These ridges display considerable variability in size; varying from 25 – 80 m in width and from 5 – 15 m in relief. We identify a series of six small moraine ridges across this sector, which record former ice margin standstills. Three of the four esker enlargements and outwash fans are observed in adjacent to a moraine.

Figure 3. Photographs detailing the morphology of the Evishanoran Esker. (A) A photograph looking east along a round-crested ridge within the complex, multi-ridge esker in the southern sector (54.571°N, -7.041°E). (B) An esker ridge within the central sector of the esker complex, formed by water flow down the hill from the right of the image (54.650°N, -6.953°E). (C) A ridge along the Esker Road within the northern sector (54.683°N, -6.942°E). Radar surveys revealed peat infilling around the ridge, masking the true esker size. (D) Large variations in ridge morphology towards the termination of the northern sector (54.734°N, -6.893°E).

Further SW (central sector), the esker transitions into a complex, arborescent system of short ridges (~0.3 km long) with more subdued relief (~6 m). This coincides with a change in the surrounding topography to greater relief variation (183 – 296 m a.s.l.) and a broadly downhill trend towards the NE. The southern end of the esker is split around a hill, with the western limb trending S-N before turning W-E, where it is cross-cut by the eastern limb, which trends N-S (Figs. 2a, 4c). The esker ridges within this sector display a dominantly simple morphology, with an enlargement only observed on a single ridge. We mapped a single moraine within this esker sector.

The southern sector consists of multiple, subparallel ridges along a slope which broadly trends downhill to the NE. While considerable variation in relief is observed due to the undulating terrain, cross-cutting relationships are absent within this sector, although ridges are observed to bifurcate (Fig. 4d). A single small esker enlargement is observed within this sector. A single, small moraine is present at the eastern end of this system.

1
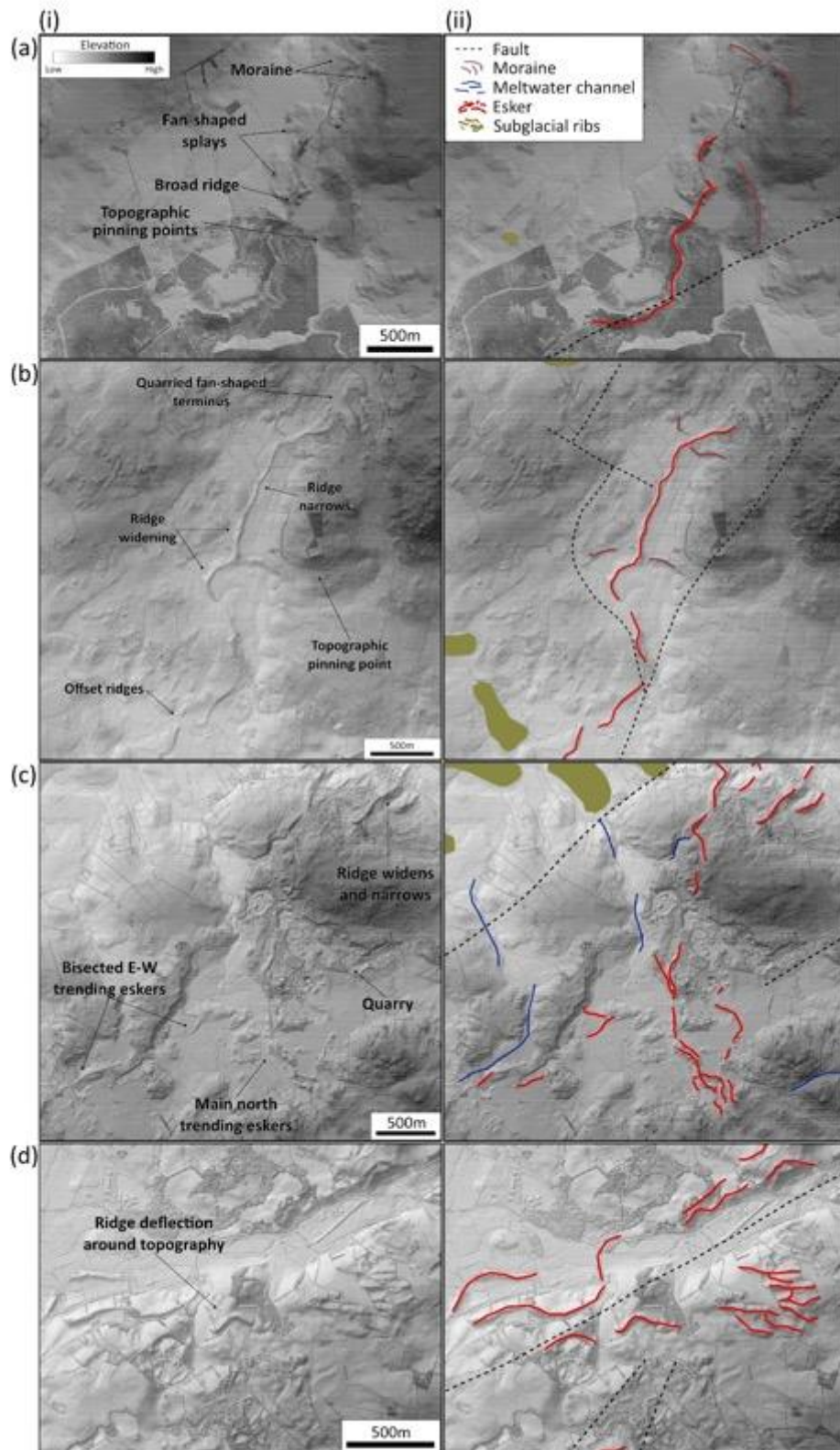
Figure 4. Hillshaded DEM detailing key morphological characteristics of the Evishanoran Esker. (a) Widening of the esker ridge towards the terminus of the simple system in the northern sector, (b) Offset ridges at the initiation of the simple system in the northern sector, (c) Cross-cutting of east trending ridges by the main north trending ridge within the complex esker system in the central sector of the esker complex, (d) Deflection of ridges around a topographic obstacle (possible bedrock or earlier drumlin) within the southern sector.

308   Complex geological faulting is observed across the study region (Fig. 2). Esker ridges commonly occur
309   near faults, while some also change orientation to follow faultlines (GSNI, 2016) (Fig. 2). This is
310   illustrated by the large fault system towards the S of the region, which trends ENE-WSW; a high
311   concentration of esker ridges within the southern sector of the esker display a spatial correspondence to
312   the fault and run subparallel to it (Fig. 4d). Individual ridges in the central sector of the Evishanoran
313   Esker are coincident with faults, where the main esker trends NE-SW towards the N of the sector.
314   Examples of correspondence between geological faults and eskers are not limited to the Evishanoran
315   Esker: to the west a small series of eskers change orientation to follow a fault which trends NW-SE,
316   highlighted in Figure 2. These changes occur three times over the ~ 5 km length of this esker.

317   *4.2 Esker Internal Architecture*

318   *4.2.1 Radar facies (RF) description and interpretation*

319   The GPR radar facies from both shielded 160MHz and unshielded 100MHz Rough Terrain antennas
320   were found to be broadly comparable (see below) and are outlined in Table 1. In this section we describe
321   facies characteristics in detail and interpret the depositional environments.

322   *4.2.1 RF1 – Coarse, poorly-bedded deposits*

323   RF1 often constitutes the core of the esker ridge, forming a tabular unit (up to 10 m thick) of
324   discontinuous, chaotic reflectors subparallel to the bed slope. The lower portion of RF1 often contains
325   hyperbola-generating point reflections. This unit is conformably overlain by RF2 or RF3, or truncated
326   by RF4 (Table 1).

327   Chaotic facies have been widely attributed to coarse, poorly-sorted deposits (Burke et al., 2008; Pellicer
328   and Gibson, 2011; Franke *et al.,* 2015; Livingstone et al., 2016; Perkins et al., 2016). This is supported
329   by sediment exposures through RF1, which comprise a variety of massive, coarse, gravelly or diamictic
330   deposits interpreted to have formed by the rapid deposition of hyperconcentrated water flows (Fig. 5c;
331   5d) (Saunderson, 1977; Gorrell and Shaw, 1991; Pellicer and Gibson, 2011; Pellicer et al., 2012;
332   Livingstone et al., 2016). Previous studies consider point reflections to represent out-of-plane boulder
333   clusters and a coarsening of material within the ridge (Burke, 2010; Burke et al., 2012). Out of plane
334   reflections (sideswipes and hyperbola) are observed to be artefacts of upstanding surface objects such
335   as trees, poles and metal farm gates (Neal, 2004). These are most notable on data from the 100MHz
336   unshielded antenna, and thus are disregarded in our interpretations.

337   *4.2.2 RF2 – Horizontally-bedded sands*

338   RF2 generally forms tabular units (~5 m thick) of continuous, subhorizontal reflectors (up to 30 m long)
339   that form parallel to the bed slope (<5° dip from horizontal). It typically forms a central unit in the esker
340   profile, regularly underlain by RF1 and draped by RF3.

341 Previous studies have attributed similar patterns of subhorizontal reflectors to a flow regime
342 characterised by vertical sediment accretion (Perkins et al., 2016). This interpretation is consistent with
343 sediment exposures through RF2 (Fig. 5a), which suggest horizontally-bedded sands deposited in a low-
344 energy glaciofluvial environment (Banerjee and McDonald, 1975; Burke et al., 2012).

345 *4.2.3 RF3 – Fine-grained, foreset deposits*

346 RF3 forms laterally constrained, wedge-shaped units (2 – 5 m thick) draped over underlying radar facies
347 (Table 1). They comprise a series of onlapping, high-angle (4° - 15° from horizontal), N to NE dipping
348 reflections. RF3 is always the topmost unit where identified and therefore represents the final stage of
349 esker building.

350 We interpret the steeply dipping reflectors as foreset beds deposited during waning flow conditions
351 (Fiore et al., 2002; Burke et al., 2008, 2010). The absence of associated backset beds suggest that
352 deposition was in a low energy environment (Burke et al., 2010). This is supported by a sediment
353 exposure located NE of a radar survey within a ridge dominated by RF3, documenting a series of fine-
354 grained, cross-stratified and downflow-dipping deposits. The lack of topset structures is indicative of
355 outwash fan-style deposits rather than a deltaic environment (Fig. 5b) (Fiore *et al.,* 2002; Winsemann
356 *et al.,* 2007).

357 *4.2.4 RF4 – Cut-and-fill basins*

358 RF4 is defined by strong, concave-upwards bounding reflectors and subhorizontal to concave internal
359 reflectors (Table 1). The bounding reflectors vary in angle, with the units ranging from narrow, steep-
360 sided basins to broader basin infills, which may extend for up to 60 m along the esker surface and reach
361 thicknesses of up to 10 m. RF4 truncates underlying facies, displaying an erosional, lower bounding
362 surface. Most frequently, RF4 is located near the surface of the esker, but in places is conformably
363 overlain by RF3. RF4 is interpreted as cut-and-fill troughs, formed during the late-stages of esker
364 genesis as water incised into the underlying sediments, and subsequently filled as flow conditions
365 waned (Gorrell and Shaw, 1991; Sambrook-Smith et al., 2006; Perkins et al., 2016).

366 Table 2. The key morphological characteristics of the complex esker system in County Tyrone. The
367 distance along the crestline of each ridge was measured to define the average ridge length. Esker
368 sinuosity was calculated for each individual ridge by dividing the esker ridge length by the straight line
369 distance from esker initiation to terminus, and is presented as a mean for each sector.

	Southern sector	Central sector	Northern sector
Planform	Complex, multi-ridge	Complex, tributary system	Simple
Average ridge length (m)	357	334	678
Sinuosity	1.17	1.21	1.2
Topographic context	Normal slope through undulating topography	Normal slope through hilly topography	Reverse slope through a uniform valley bottom
Relative relief (m)	~7	~6	~10-15
Total esker length (km)	~6.5 (36 ridges)	~7.4 (39 ridges)	~9.3 (10 ridges)

370

371 *4.2.5 RF5 – Post-glacial infill*

372 Present along the flanks in cross-profile surveys of esker ridges, RF5 is separated from the main esker
373 ridge elements by a strong bounding surface, which dips steeply away from the esker (Table 1). The
374 interior of these units is strongly attenuated and characterised by homogenous reflections which are
375 broadly horizontal. RF5 is interpreted as postglacial infill of the area surrounding the esker ridge. The
376 reflection patterns are consistent with that of peat, which is prevalent across Ireland and confirmed by
377 observations in the field (Jol and Smith, 1991; Pellicer *et al.,* 2012).
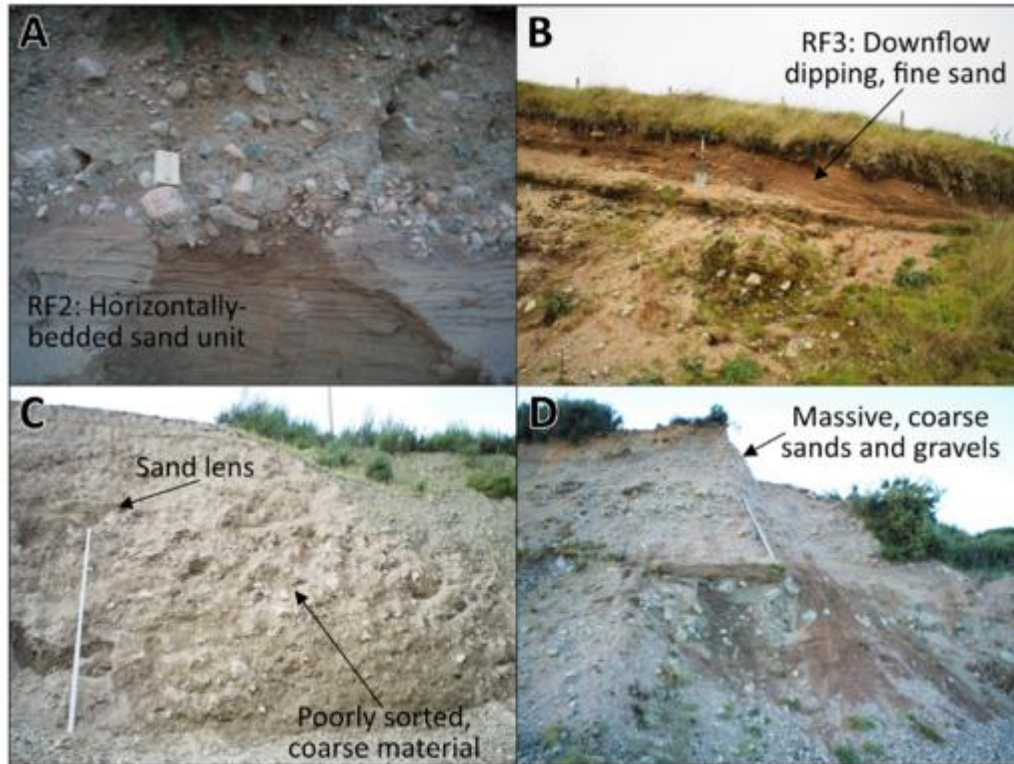
378 Figure 5. (a) Sediment exposure from the southern-end of the northern sector, consisting of a series of
379 horizontally stratified sands, overlain by a massive gravel unit (54.668°N, -6.950°E). (b) Sediment
380 exposure within the central, complex esker system, dominated by a series of fine-grained, downflow-
381 dipping fan deposits associated with RF3 (54.650°N, -6.953°E). (c) Quarried section of the single esker
382 ridge system to the north of (a). Facies consist of coarse, diamictic material with boulders up to 50 cm
383 (54.672°N, -6.941°E). (d) Massive sand and gravel units observed within the northern sector, commonly
384 associated with RF1 (54.668°N, -6.950°E).

385 *4.3 Site architecture*

386 At each site, radar profiles were divided into radar facies according to Table 1 and Section 4.2 above.
387 Here we describe the architecture of individual esker ridges and outline the processes responsible for
388 their formation.

389 *4.3.1 Site 1*

390 Site 1 is a 1.6 km long, broad, round-crested esker ridge at the northern termination of the single ridge
391 esker system (northern sector). We conducted a 0.9 km, 100 MHz radar survey along a road following
392 the crest of the esker ridge (Fig. 6). The ridge is situated along a forest-covered valley bottom on a slope
393 that dips towards the southwest and is significantly wider than southerly ridges within the system (up
394 to 140 m wide and 16 m high). The esker surface displays minor undulations (<1 m over ~ 90 m).

395 The architecture of the esker ridge is defined by a semi-continuous bounding surface with varying
396 elevation along the upper part of the radar profile (Fig. 6). Below this bounding surface is a core of RF1

2

present along the whole esker profile. The chaotic reflections suggest coarser material with a lack of structure, so are interpreted to have formed by rapid deposition during high flow velocities (Burke *et al.,* 2010; Pellicer and Gibson, 2011; Franke *et al.,* 2015; Livingstone *et al.,* 2016). At around 500 m along the profile, side-swipes are observed, likely relating to signal scattering from surface obstacles (Cassidy and Jol, 2009). No lower bounding surface is observed for this unit, but a maximum thickness of 15 m is present at ~ 600 m. Towards the esker surface, the semi-continuous bounding surface defines units of RF4 from 250 m onwards. The concave basin-infills (RF4) vary in size, up to ~ 6 m deep and ~ 80 m wide. At multiple locations the contact with RF4 and underlying reflectors is erosional (Fig. 6). The reflectors observed in these concave infills are less chaotic, which we interpret to have formed as cut-and-fill features, with deposition of finer sediment during waning flow (Sambrook-Smith *et al.,* 2006; Franke *et al.,* 2015; Table 1). Cut-and-fill structures observed in eskers have previously been interpreted to occur when thermomechanical excavation is outweighed by creep closure, leading to increased flow velocities and the erosion of underlying sediments (Perkins *et al.,* 2016).

4.3.2 Site 2

Fig. 7 shows a 0.6 km, 160 MHz radar profile taken along the crest of a 1.9 km long, round-crested ridge, near the southern end of the simple esker system (northern sector). Fig. 8 displays a cross-profile (including a short long-profile section of the crestline), taken from just over halfway along the ridge. The topographic context of the system is largely uniform, with the ridge trending up a reverse bed slope along the valley floor. The ridge morphology varies along its length. Undulations (up to 2 m high) are observed to be associated with esker widening, and the ridge generally becomes smaller towards the north (downflow), terminating in a fan-shaped deposit.

419
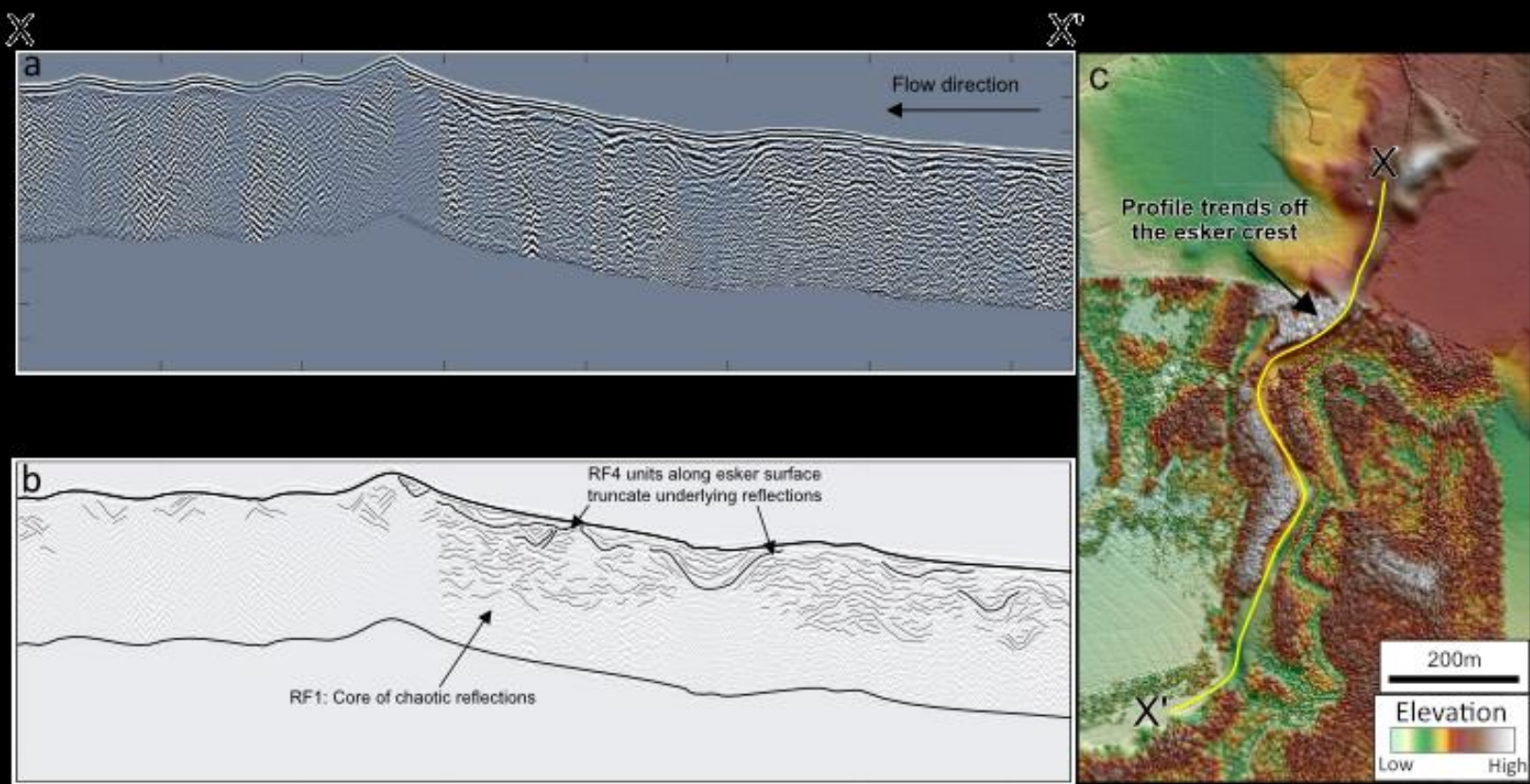
Figure 6. (a)100 MHz long-profile radar survey along the crest of a single ridge esker towards the NE terminus of the County Tyrone Esker, the location of the survey line is presented in Fig. 2. Ice flow direction is indicated by the black arrow. (b) shows an interpreted radar profile derived through the tracing of key reflections. (c) Inset figure showing the detailed esker morphology and the location of radar survey (yellow line).

423

424
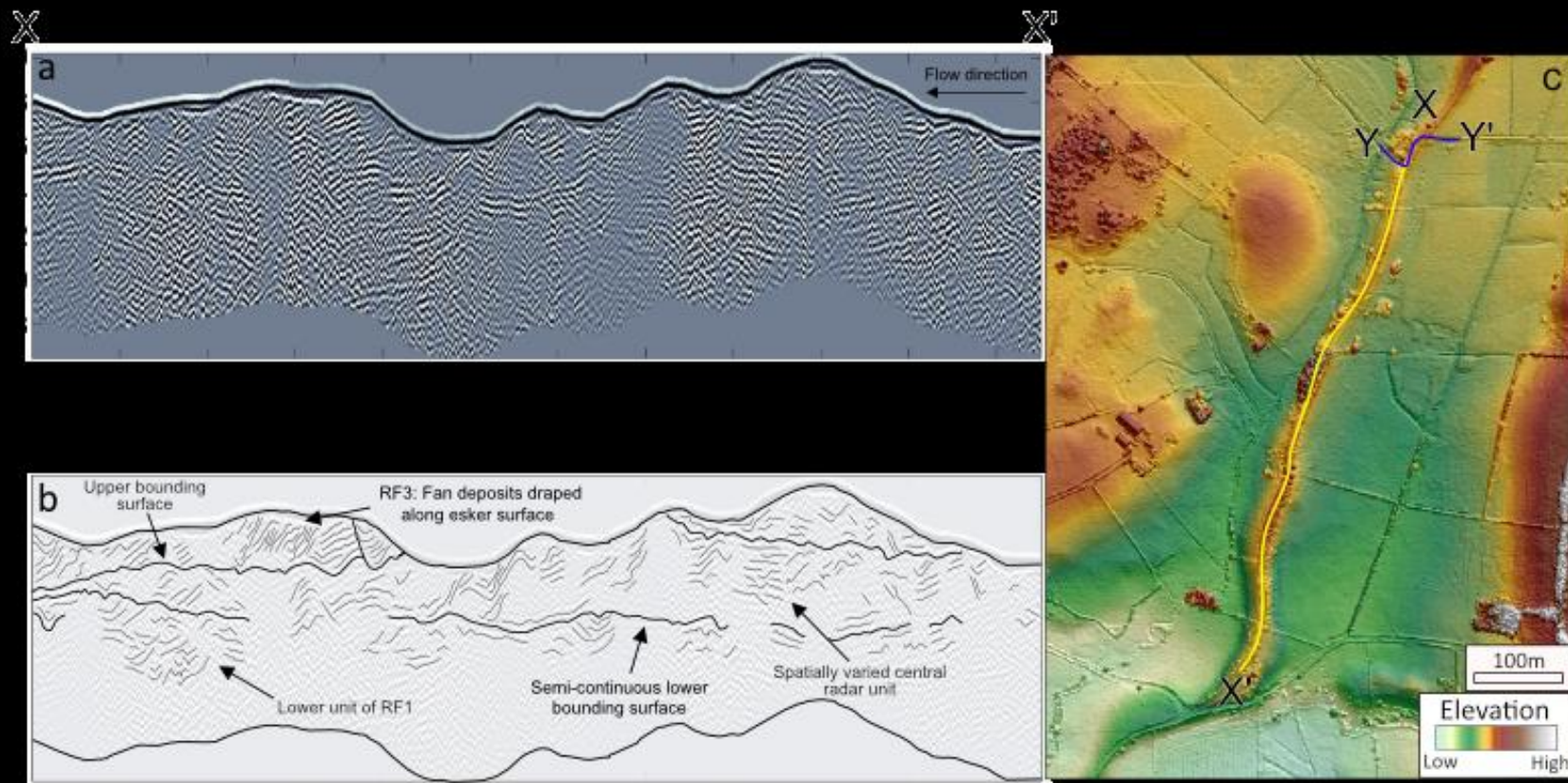
Figure 7. (a) 160 MHz long-profile radar survey along the crest of a single ridge esker near the initiation of the simple system, the location of the survey line is presented in Fig. 2. Ice flow direction is indicated by the black arrow. (b) shows an interpreted radar profile derived through the tracing of key reflections. (c) Inset figure showing the detailed esker morphology and the location of radar survey for figure 7 (yellow line) and the radar survey line for figure 8 (blue line).
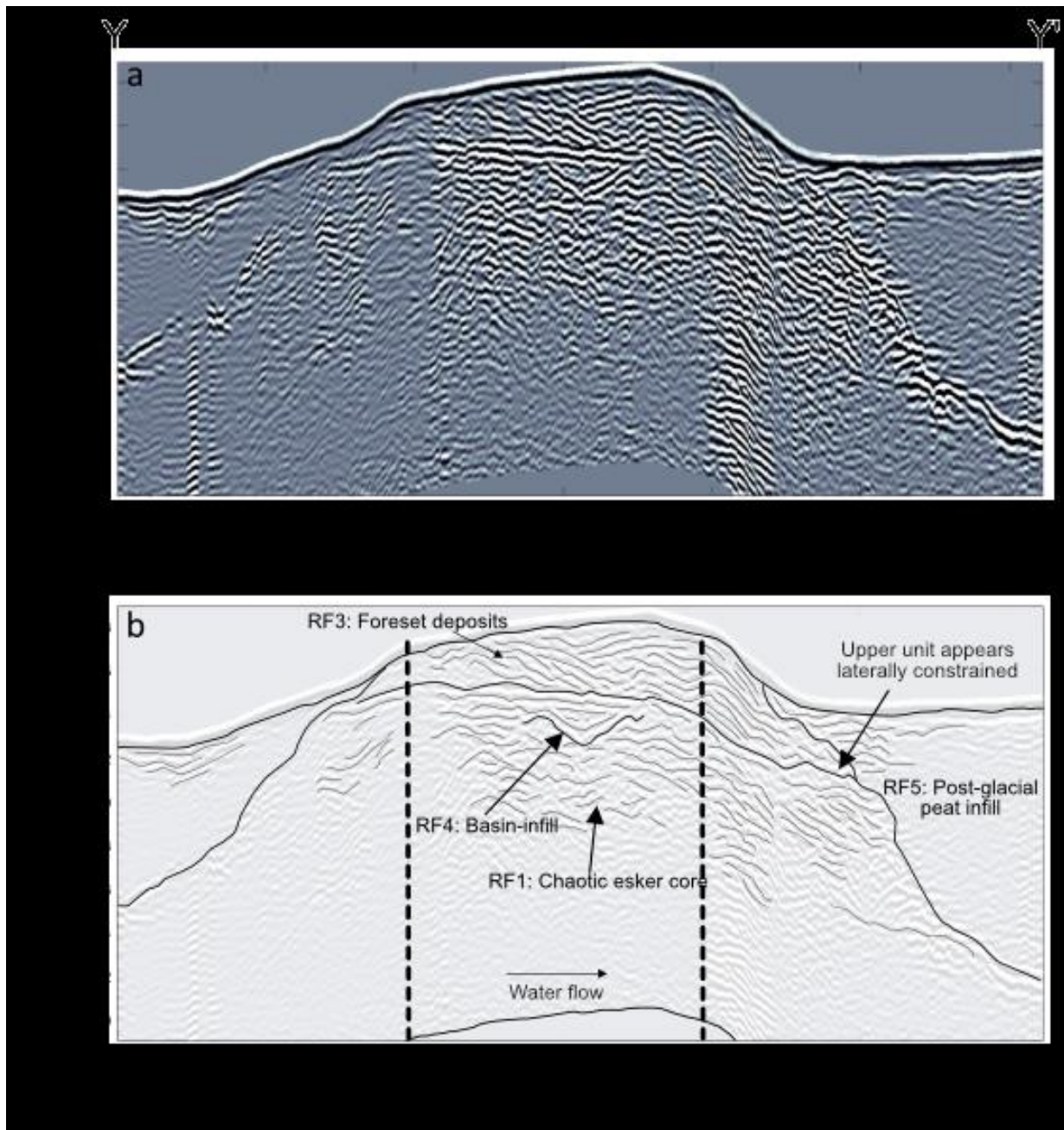
Figure 8. (a) 160 MHz long-profile radar survey along the crest of a single ridge esker near the initiation of the simple system, the location of the survey line is presented in Fig. 2. Ice flow direction is indicated by the black arrow. (b) shows an interpreted radar profile derived through the tracing of key reflections, vertical dashed lines indicate the portion of the radar survey which travelled along the esker ridge. The location of the radar profile is indicated on Fig. 7c by a blue line.

1
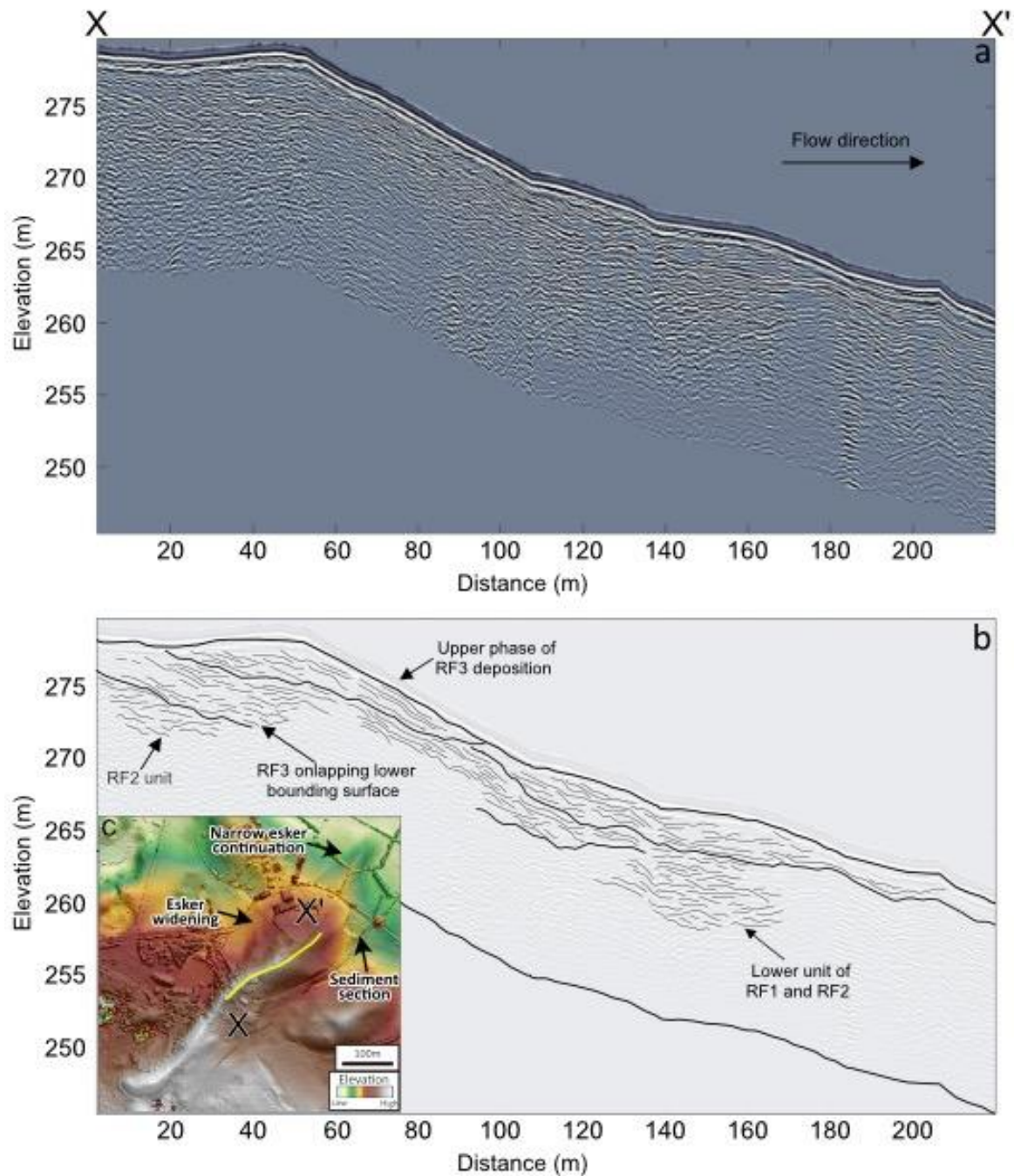
Figure 9. (a) 160 MHz radar profile along the crest of an esker within the complex central sector. The red line indicates the radar survey location and the white dot shows the photograph location in Fig. 5b. Ice flow direction is indicated by the black arrow. (b) shows an interpreted radar profile derived through the tracing of key reflections, vertical dashed lines indicate the portion of the radar survey which travelled along the esker ridge. (c) Inset figure showing the detailed esker morphology and the location of radar survey (yellow line), while the labelled sediment section is photographed in Fig. 5b.
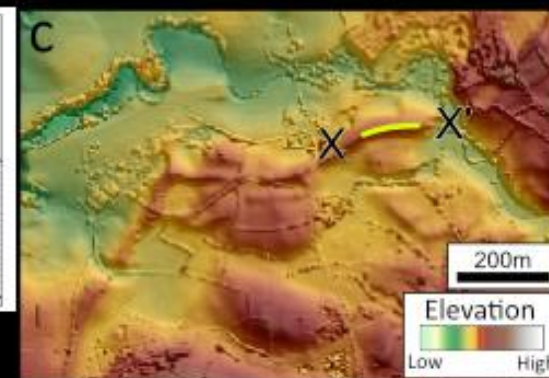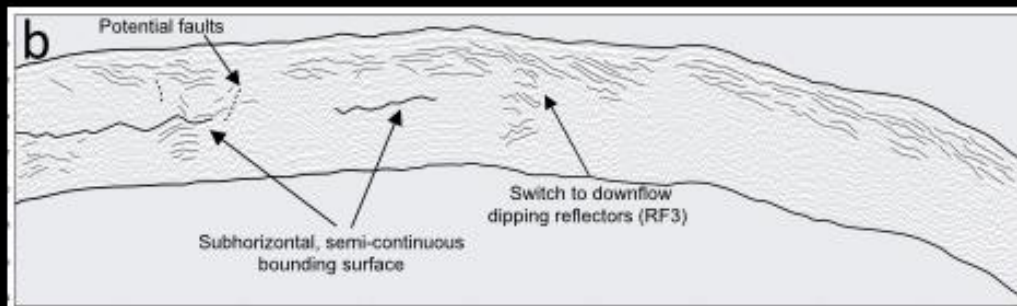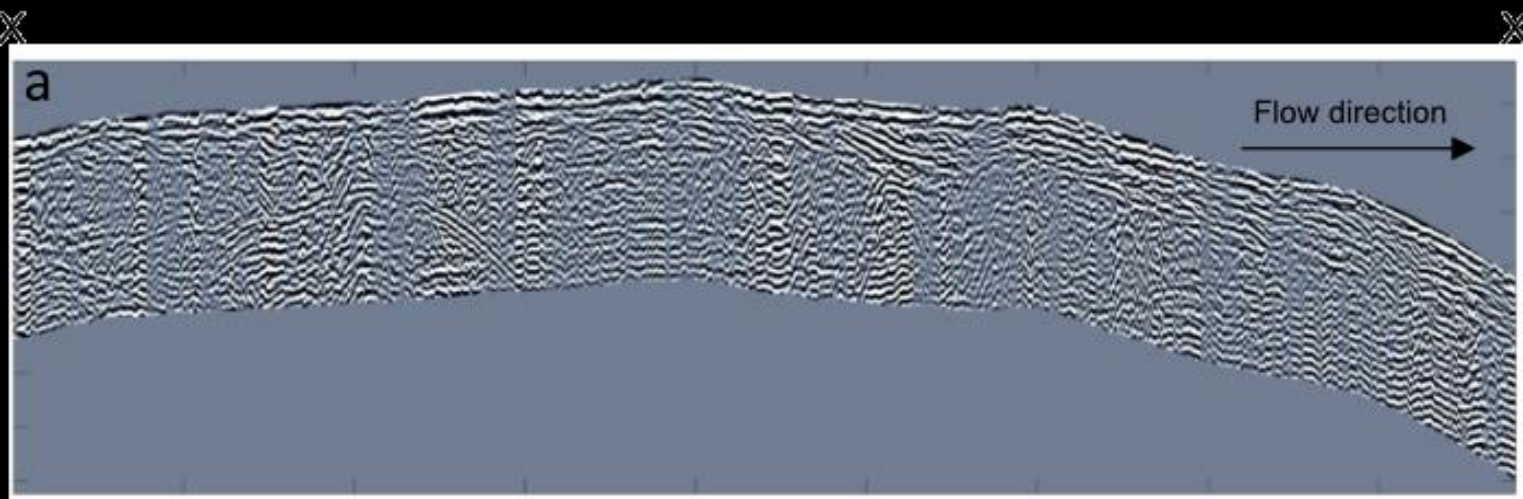
Figure 10. (a) 160 MHz radar profile along the crest of an esker within the southern sector. Ice flow direction is indicated by the black arrow. (b) shows an interpreted radar profile derived through the tracing of key reflections, vertical dashed lines indicate the portion of the radar survey which travelled along the esker ridge. (c) Inset figure showing the detailed esker morphology and the location of radar survey (yellow line).

1

Two strong, horizontal bounding reflectors divide the ridge into three architectural units. These bounding surfaces are discordant with the undulating esker surface. The lowest bounding surface is observed at ~224 m elevation, with the underlying unit comprising a core of RF1 (present along the length of the profile). Variations in thickness (~1 - 4 m) are observed, although no clear esker base is identified. Between 0 - 10 m distance, a single unit of RF4 is present, cutting into RF1 with a depth of ~1 m. This lower radar element relates to the initial stages of esker formation, and indicates high flow energy and deposition of coarse material (Pellicer and Gibson, 2011; Livingstone *et al.,* 2016). Above the bounding surface at ~224m elevation, the radar facies of the central unit varies spatially. Chaotic reflections (RF1) dominate the upflow section from 400 – 550 m distance. Moving downflow, these reflections become more continuous and in places exhibit a downflow dip (RF3; ~ 250m distance). Above the upper bounding surface (225 m elevation), a ~2 m thick, tabular unit of RF3 is continuous between 0 – 200 m distance, but absent from 200 – 400 m distance. The presence of RF3 indicates a switch to waning flow conditions in a progradational depositional environment. This unit is draped along the esker crest and does not extend over the esker flanks, coinciding with an increase in esker height, this suggests that deposition was constrained by ice walls (Fig. 8). Foreset-backset macroforms have been associated with dynamic subglacial conduit enlargements during high flow energy conditions (Fiore *et al.,* 2002; Burke *et al.,* 2010). The absence of backset deposits within this esker suggests another mechanism was responsible for the change to progradational deposition.

Between 400 - 500 m distance, another radar element is draped over the esker surface, consisting of subhorizontal to chaotic reflections (RF1 and RF2), coincident with an undulation and widening of the esker ridge. Overall, esker architecture records a transition from high-energy flow during the initial stages, to waning flow conditions where depositional processes reflect local ice tunnel conditions. In cross-profile, up to 8 m of post-glacial peat deposition (RF5) is documented on the esker flanks. This may result in less than 50% of the true esker height being observable at the surface (Jol and Smith, 1991; Pellicer et al., 2012).

4.3.3 Site 3

Fig. 9 presents a 0.2 km, 160 MHz radar profile along the crest of a 0.8 km round-topped esker ridge, within the complex multi-ridge system (central sector). The ridge is situated in an area of steep, hilly topography. At ~300m along the esker morphology develops from a narrow ridge (~50m wide) into a broad, fan-shaped enlargement which is ~130m wide and ~250m long, before the ridge terminates in a narrower section (~50m wide) that is ~200m long in an open topographic basin that drains to the northwest. The radar profile starts on the summit of a hill at the beginning of the enlargement and then follows the esker crest downslope (Fig 9). Three other ridges are located adjacent to the studied esker, terminating in the same basin. A gravel pit is located at the terminus of the ridge, consisting of a series of sand and gravel foreset units which dip to the northeast (Fig. 5b).

480 Within the lowest radar unit, between 0 – 40 m distance, the sequence is dominated by at least 3 m of
481 coherent horizontal reflections (RF2) indicating vertical accretion of fine material (Burke *et al.,* 2012).
482 Poor radar penetration prevents the identification of the lower bounding surface of this unit. From 120
483 – 170 m along flow, a unit up to 7 m thick, composed of more discontinuous reflections (RF1 and RF2)
484 represent a lateral transition to coarser material lacking structure, interpreted to be deposited
485 subglacially under higher flow energy (Pellicer and Gibson, 2011; Franke *et al.,* 2015; Livingstone *et*
486 *al.,* 2016). The upper section of the radar profiles is dominated by units of wedge-shaped units
487 composed of continuous downflow dipping reflectors. From 0 – 140 m, the units of RF3 are onlapping,
488 but 140 m onwards is characterised by a single unit of RF3 along the surface. These upper units likely
489 represent a series of foresets and cross-stratified sands and gravels, deposited during low flow energy
490 conditions in a progradational environment (Franke *et al.,* 2015). We interpret this onlapping sequence
491 of foresets, composed of cross-stratified sands and gravels, as an outwash fan deposited as meltwater
492 exits a subglacial conduit at the ice sheet margin (Winsemann *et al.,* 2007). This is supported by the
493 transition to a broader, fan-shaped morphology of the esker enlargement that suggests this outwash fan
494 may be superimposed on a core of material that was deposited subglacially (Fig. 9).

495 *4.3.4 Site 4*

496 Fig. 10 shows a 0.18 km long, 160 MHz radar profile along part of the crest of a 0.75 km round-crested
497 esker within the complex, multi-ridge to anabranching esker system (southern sector). The esker system
498 is situated in an area of complex, hilly topography. The general esker trend is subparallel to a fault-
499 controlled valley, with ridges situated in and around it (Fig. 5d).

500 A single bounding surface is semi-continuous along the radar profile, present from 0 – 70 m distance,
501 at an elevation of ~ 233 m (Fig. 10). Below this bounding surface, a ~2 m thick core unit of chaotic
502 reflections (RF1) is present in sections of the radar profile where penetration was deep enough. These
503 chaotic reflections suggest the presence of coarse material deposited under high energy flow conditions
504 (Pellicer and Gibson, 2011; Livingstone *et al.,* 2016). Above the bounding surface, the radar units (~4m
505 thick) comprise of more continuous reflections which either subhorizontal or downflow dipping (RF2
506 and RF3). This represents an increase in structure as finer material was deposited during waning flow
507 conditions (Franke *et al.,* 2015). The upflow section (0 - 80 m distance) is dominated by RF1 and RF2,
508 while the downflow section (80 m distance onwards) consists of more coherent units of RF3. This
509 transition to fine-grained foresets (RF3) coincides with a change to a downslope trend.

510 **5.0 Discussion**
511 The following section seeks to further our understanding of esker formation based on the sedimentary
512 architecture of a morphologically diverse esker system. First, the broad-scale architecture is considered
513 in order to develop a depositional model of esker formation. Second, local controls on esker formation

514   and morphology are discussed. Finally, we use our findings to reconstruct the ice sheet retreat pattern
515   and retreat rate for the Omagh Basin region.

516   5.1 Esker formation

517   a.   A two-phase model of esker deposition

518   The Evishanoran Esker has a broadly homogeneous large-scale sedimentary architecture, despite
519   changes in esker morphology and topographic context (Figs. 6-10). GPR surveys reveal two main
520   phases of esker formation. Initial esker growth involved deposition of coarse gravel or diamict from
521   subglacial hyperconcentrated flows, which may have occurred in a somewhat synchronous manner
522   (Saunderson, 1977; Gorrell and Shaw, 1991; Pellicer and Gibson, 2011). Although, offset ridge
523   relationships and eskers terminating in fans in the northern sector suggest that this deposition likely
524   extended for a maximum of a few kilometres up-ice, rather than tens of kilometres (Fig. 4b). Later
525   stages of esker growth coincide with a transition to well-sorted, fine-grained deposits as flow energy
526   wanes (Franke *et al.,* 2015). Radar facies document a variety of hydrological processes during this final
527   phase of formation (RF2, RF3 and RF4), in contrast to the simple earlier phase dominated by
528   hyperconcentrated flows (RF1).

529   As meltwater approaches the ice sheet margin, subglacial conduits experience reduced creep closure
530   (reaching zero at the ice margin: Rothlisberger, 1972). Despite this, thermomechanical excavation
531   continues to enlarge the subglacial conduit, meaning that the subglacial conduit grows towards the ice
532   sheet margin (Drews *et al.,* 2017). This expansion of the subglacial conduit is expected to cause a
533   progressive reduction in flow energy towards the ice sheet margin (Hewitt and Creyts, 2019). This
534   causes a reduction of the carrying capacity and the deposition of well-sorted, finer material. Therefore,
535   sedimentation rates are highest at the ice sheet margin. This results in an enlargement of the esker profile
536   at or near to former ice margin standstills (Fig. 11a). Additionally, as meltwater exits the subglacial
537   conduit at the ice sheet margin, flow expansion will result in a rapid fall in flow energy and the formation
538   of outwash fans and foreset deposits.

539   Esker size, and the thickness of stratigraphic units, is dependent on the duration of deposition and the
540   rate of deposition. As we described, the deposition rate is likely linked to the proximity of a location to
541   the ice sheet margin, as well as rates of sediment supply. While the duration of deposition will be related
542   to the rate of ice sheet margin retreat. Rapid margin retreat will reduce the time available for deposition,
543   while a standstill will result in enhanced deposition at and near the ice sheet margin. Therefore, we
544   suggest that enlargements in the esker profile can indicate a former ice margin position. Under a stable
545   ice sheet margin position, we would expect a simple esker profile which grows in size towards it's
546   terminus. However, variations in the retreat rate during deglaciation will lead to the superimposition of
547   later esker deposits during time-transgressive esker formation (Fig. 11b). We suggest the observed esker
548   enlargements are a form of esker bead deposited at the ice sheet margin, and superimposed on the core

3

549 of subglacially deposited coarser material during a two-phase time-transgressive depositional model

550 (Fig. 7, 9 and 11) (Livingstone *et al.,* 2020).

551 Enlargements in eskers or outwash fans are commonly observed across the Evishanoran Esker. We

552 suggest these enlargements can be used to reconstruct the relative ice sheet margin retreat rate and

553 former ice margin positions. We favour enlargement formation at the ice sheet margin, over the

554 possibility of formation in an enlargement within the subglacial conduit, as we do not observe a backset-

555 foreset macroform which is diagnostic of this formation (Burke *et al.,* 2015). Caution must be taken

556 when using these to reconstruct the retreat rate, as variations in sediment supply may also influence the

557 development of these enlargements. But, the common co-occurrence of esker enlargements with

558 topographic pinning points (Fig. 4a) or moraines (Fig. 4b) supports an ice marginal origin for esker

559 enlargements.

560 Morphogenetic relationships have been proposed for eskers on the southern Fraser Plateau, British

561 Colombia (Burke *et al.,* 2015; Perkins *et al.,* 2016), while esker complexity has been related to

562 meltwater flow conditions and sediment supply in Svalbard and Iceland (Storrar *et al.,* 2015, 2020). In

563 central Northern Ireland, the relationship between esker morphology and the depositional processes is

564 less clear. At the local scale, undulations and enlargements of the esker profile appear to relate to a two-

565 phase depositional model during ice sheet retreat. An esker core is formed by synchronous subglacial

566 deposition, while enlargements are formed by the time-transgressive deposition of fine sediment near

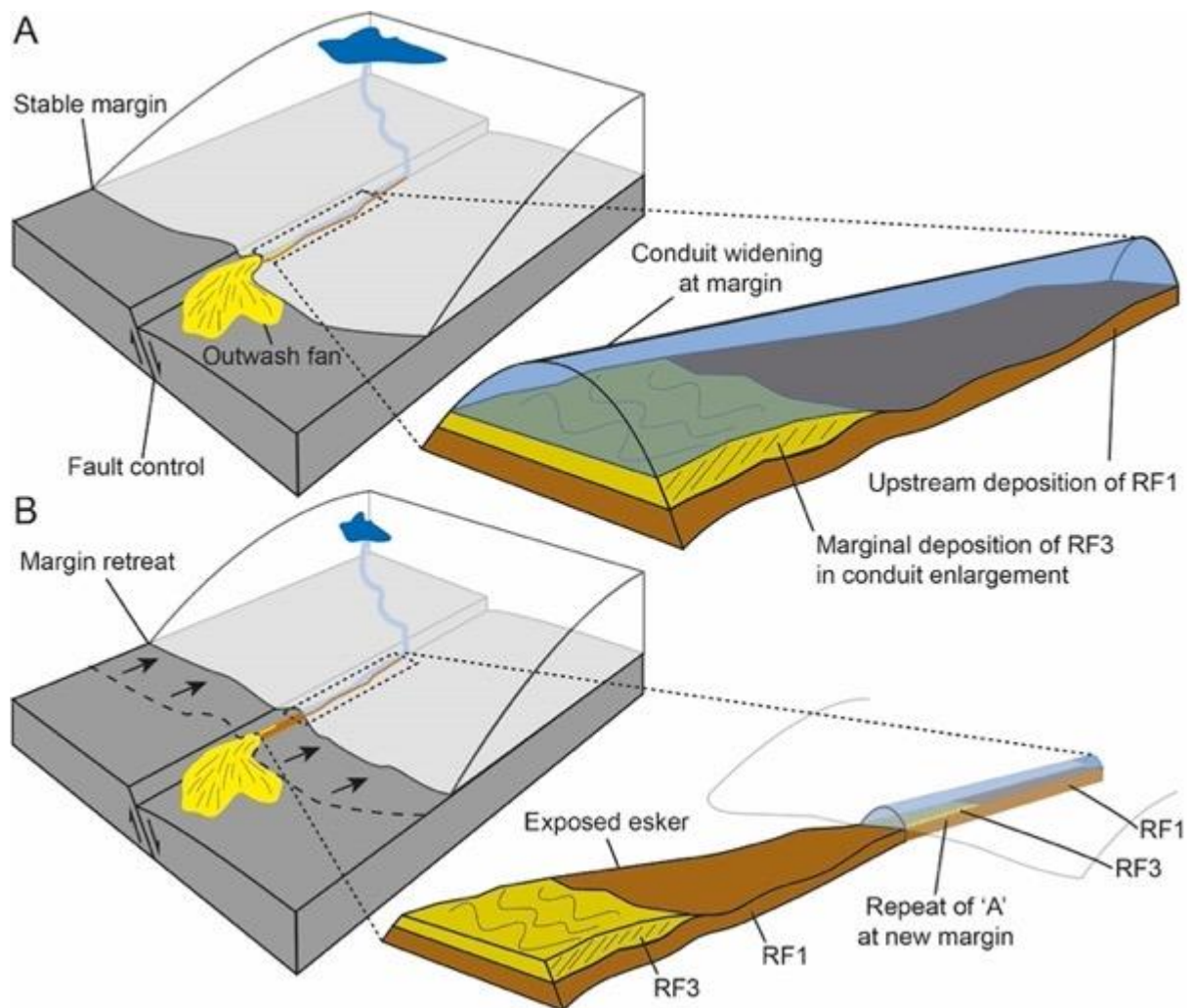567 to the ice sheet margin (Fig. 11).

Fig. 11. A conceptual model of the two-phase esker deposition. (a) Outwash fans and foresets are deposited at the ice sheet margin due to conduit widening, while coarser material is deposited up-ice in the subglacial conduit. (b) Ice margin retreat leads to the deposition of foresets or outwash fans on top of the core of esker material.

b. Local controls

The morphology of eskers is influenced by the overall drainage characteristics during formation (Burke *et al.,* 2015; Storrar *et al.,* 2015), as well as local factors (Clark and Walder, 1994; Storrar *et al.,* 2014a; Knight, 2019). Beneath the Laurentide Ice Sheet, complex eskers are more common in areas of greater topographic variability (Storrar *et al.,* 2014a). In the Evishanoran Esker, a similar relationship between complex morphology and topography is observed. At the large-scale, the complex southern and central esker planforms are associated with a topographic context dominated by high variations in relief, while the simpler northern sector is located on the bottom of a broad valley floor. The distribution of eskers in the central sector clearly illustrates this topographic influence, as eskers are deflected around the ~100m hill (Fig. 4c). We propose that esker complexity in central Northern Ireland is largely controlled by the topographic variability. Undulating topography may cause the subglacial conduit to fragment around obstacles or migrate as ice thinned (Wright *et al.,* 2008; Storrar *et al.,* 2014).

5

584   The complexity of esker systems in areas of high topographic variability reflects a combination of
585   spatial and temporal changes in the subglacial drainage network. Within the central sector of the
586   Evishanoran Esker, the cross-cutting esker patterns suggest that the drainage system evolved over time
587   to create the complex esker network as the drainage pathways migrated during deglaciation (Fig. 4c).
588   In contrast, the anabranching nature of the southern sector, with no cross-cutting relationships may
589   instead represent a drainage network which is fragmented by the complex topography (Fig. 4d). This is
590   supported by the association with a series of meltwater channels cut into, and ascending, the hill to the
591   south of this sector (Fig. 2b), which may have been active at similar times. Pressurised meltwater eroded
592   the meltwater channels on the southern slopes of the hill. Reductions in pressure on the downslope trend
593   then led to the deposition of the esker system (Livingstone et al., 2016). It is also possible that increased
594   deposition on the downslope trend may have led to channel clogging and avulsion (Storrar *et al.,* 2015).

595   Substrate characteristics have been hypothesised to influence the formation and distribution of eskers.
596   Eskers are more common on more resistant bedrock (Clark and Walder, 1994), while esker morphology
597   in north-central Ireland is controlled by a variety of substrate factors, including the influence of pre-
598   existing glacial features (Knight, 2019). The transition from sandstone and limestone in the south to the
599   crystalline granites in the north does not appear to influence esker distribution in the region south of the
600   Sperrin Mountains. However, a high level of spatial correspondence between eskers and geological
601   faults is observed (Fig. 2). This correspondence includes eskers in the southern sector running sub-
602   parallel to a large fault-controlled valley, and pronounced changes in the orientation of eskers to trend
603   along faults (Fig. 2). Enhanced groundwater flow along zones of higher transmissivity (e.g. faults) may
604   influence the distribution of the subglacial drainage system (Boulton *et al.,* 2007a; 2007b; 2009). In
605   central Northern Ireland, this relationship appears to strongly control the subglacial drainage network.

606   The morphometry of eskers may relate to a combination of sediment and meltwater supply (Shreve,
607   1985; Storrar *et al.,* 2015), but caution must be taken when using solely geomorphological observations
608   of eskers to investigate the hydrological system of a palaeo-ice sheet. Radar surveys revealed substantial
609   post-glacial peat infilling around eskers, reducing the relative relief of eskers in the northern sector. The
610   relative relief of one esker is 5 m, but with up to 6 m of esker deposits hidden below the surface (Fig.
611   8). Extensive peat deposits have been documented in the Irish Midlands, up to 5.5 m thick (Pellicer and
612   Gibson, 2011; Pellicer *et al.,* 2012), which must be taken into consideration when using esker
613   dimensions to gain an insight into glacial history.

614   5.2 Implications for deglaciation of Northern Ireland

615   Three main ice dispersal centres operated during the deglaciation of the north of Ireland. This includes
616   an upland ice dispersal centre in the Donegal Mountains, and lowland ice domes in the Lough Neagh
617   and Omagh basins, which have been well documented in previous literature (Knight, 1997; Knight and
618   McCabe, 1997; McCarron, 2013). Across this region, meltwater landforms and small moraines record

619   the final retreat pattern of the Irish Ice Sheet. Here we describe the broader retreat patterns of the Irish

620   Ice Sheet, before using the Evishanoran Esker to describe the retreat rate of the Omagh Basin ice.

621   These ice domes were coalescent at the start of deglaciation, indicated by subglacial bedform patterns

622   (Fig. 2a), but became isolated ice domes followed ice sheet thinning and saddle collapse. Eskers

623   oriented radially around the Lough Neagh basin record the final retreat pattern inwards. Lough Neagh

624   ice separated from the Lough Erne/Omagh Basin ice dome along an approximately N-S axis located to

625   the south of the eastern Sperrin Mountains (Fig. 2a). In the west, the Lough Erne ice dome separated

626   from ice sourced from the Donegal and Sligo Mountains sometime between 15-16ka, according to the

627   isochrons of Wilson *et al.* (2019). Lateral meltwater channels record the downwasting of ice flowing

628   from Sligo and Donegal into the Lough Erne Basin, recording when summits became ice-free and the

629   separation of these ice dispersal centres. The position of these channels suggests Donegal ice flowed

630   into the Lough Erne Basin, indicating that Donegal ice persisted long enough to flow into a mostly

631   deglaciated Lough Erne Basin (Fig. 2b). This is consistent with dating evidence that suggests that the

632   Donegal Mountains held the final remnants of the British-Irish Ice Sheet (Wilson *et al.,* 2019).

633   The relative retreat rate and former ice margin standstills can be identified from the morphology of the

634   Evishanoran Esker and associated landforms. The initial southwards ice margin retreat from the Sperrin

635   Mountains was quite slow across the northern esker sector. We identify at least four former ice margin

636   standstills over the 9.3 km this sector spans, from evidence of five small moraines, two esker

637   enlargements, three outwash fan deposits and sedimentological information (Fig. 2b,c). These former

638   standstill locations are mostly located at topographic pinning points. The retreat rate was more rapid

639   across the central sector. A single moraine and outwash fan at the northern end of this sector suggest

640   only one standstill, due to their close proximity, across the 7.4 km sector length. The retreat rate across

641   the southern sector may have slowed slightly, as the retreat direction became oriented towards the SW.

642   Geomorphological evidence suggests one or two possible standstills over a distance of 6.5 km. A small

643   moraine at the north-eastern side of the sector suggests a standstill at the start of esker formation in this

644   sector, where a hill (~150m relative relief) may have acted as a pinning point. A small enlargement

645   associated with foreset deposits may have formed under a short-lived standstill in the centre of this

646   sector (Fig. 10). However, the retreat was likely more rapid than in the northern sector due to the

647   relative lack of geomorphological evidence.

648   *6.0 Conclusions*

649   The Evishanoran Esker was deposited time-transgressively in a subglacial, closed conduit or at the ice

650   sheet margin and records the final stages of ice retreat in this region from the Sperrin Mountains to the

651   south. Esker distribution is a result of the dynamic evolution of the subglacial hydrological system, and

652   does not record an extensive drainage network. Based on our observations, we present a series of key

653   points regarding the deglacial history and broader implications for esker formation:

7

1. Deposition of the Evishanoran Esker occurred in two main flow phases. An initial phase of semi-synchronous, subglacial deposition formed the esker core. A second phase of time-transgressive deposition near the ice sheet margin. This occurs as the subglacial conduit enlarges due to reduced creep closure, causing an increase in deposition of fine material and foresets. Esker enlargements occur where these time-transgressive deposits are observed, and can indicate former ice margin positions.

2. The internal architecture of eskers is broadly homogenous across all sectors, suggesting that hydrological conditions are largely comparable across the sectors. Variations in esker morphology cannot solely attributed to variations in drainage characteristics. Instead we suggest local topographic conditions influence esker complexity.

3. Using evidence for former ice margin standstills we reconstruct the variations in the retreat rate across the Evishanoran Esker. Ice margin retreat across the northern sector was slow, with retreat rate increasing during margin retreat across the central and southern sectors.

4. Geologic and topographic settings control esker distribution and formation. The close association between the orientation and distribution of eskers and faults suggest that underlying geological structural weaknesses act as a zone of high meltwater transmissivity. The reconstruction of ice dynamics from meltwater features must also consider the influence of local factors on distribution.

5. Post-depositional processes can have a significant influence on esker geomorphology. Post-glacial fluvial erosion has previously been invoked to explain the fragmentation of some esker systems. We identify significant post-glacial peat infilling which masks esker dimensions and poses a problem for esker studies that rely solely on remote sensing morphometric analysis.

References

Alley, R.B., Blankenship, D.D., Bentley, C.R. and Rooney, S.T. (1986) Deformation of till beneath ice stream B, West Antarctica. Nature 322, 57-59.

Aylsworth, J.M. and Shilts, W.W. (1989) Bedforms of the Keewatin ice sheet, Canada. *Sedimentary Geology*, *62*(2-4): 407-428

Banerjee, I. and McDonald, B.C. (1975) Nature of esker sedimentation, in Jopling, A. V., and McDonald, B. C., eds., Glaciofluvial and glaciolacustrine sedimentation: Society of Economic Paleontologists and Mineralogists Special Publication No. 23: 132-154.

Bartholomew, I., Nienow, P., Mair, D., Hubbard, A., King, M.A. and Sole, A. (2010). Seasonal evolution of subglacial drainage and acceleration in a Greenland outlet glacier. Nature Geoscience, 3(6), 408-411.

Bell, R.E., Studinger, M., Shuman, C.A., Fahnestock, M.A. and Joughin, I. (2007). Large subglacial lakes in East Antarctica at the onset of fast-flowing ice streams. Nature, 445(7130), 904-907.

Boulton, G.S., Lunn, R., Vidstrand, P. and Zatsepin, S., (2007a) Subglacial drainage by groundwater-channel coupling, and the origin of esker systems: part 1—glaciological observations. *Quaternary Science Reviews*, *26*(7-8), 1067-1090

Boulton, G.S., Lunn, R., Vidstrand, P. and Zatsepin, S. (2007b) Subglacial drainage by groundwater–channel coupling, and the origin of esker systems: part II—theory and simulation of a modern system. *Quaternary Science Reviews*, *26*(7-8), 1091-1105

Boulton, G.S., Hagdorn, M., Maillot, P.B. and Zatsepin, S. (2009) Drainage beneath ice sheets: groundwater–channel coupling, and the origin of esker systems from former ice sheets. *Quaternary Science Reviews*, *28*(7-8), 621-638

Bradwell, T., Stoker, M.S., Golledge, N.R., Wilson, C.K., Merritt, J.W., Long, D., Everest, J.D., Hestvik, O.B., Stevenson, A.G., Hubbard, A.L. and Finlayson, A.G. (2008) The northern sector of the last British Ice Sheet: maximum extent and demise. *Earth-Science Reviews*, *88*(3-4): 207-226

Brennand, T. A. (1994). Macroforms, large bedforms and rhythmic sedimentary sequences in subglacial eskers, south-central Ontario: implications for esker genesis and meltwater regime. *Sedimentary Geology*, *91*(1–4), 9–55. https://doi.org/10.1016/0037-0738(94)90122-8

Brennand, T.A. (2000) Deglacial meltwater drainage and glaciodynamics: inferences from Laurentide eskers, Canada. *Geomorphology*, *32*(3-4): 263-293

Budd, W.F., Keage, P.L. and Blundy, N.A (1979). Empirical studies of ice sliding. Journal of Glaciology, 23, 157-170.

Burke, M. J., Brennand, T. A., & Sjogren, D. B. (2015). The role of sediment supply in esker formation and ice tunnel evolution. *Quaternary Science Reviews*, *115*, 50–77. https://doi.org/10.1016/j.quascirev.2015.02.017

Burke, M. J., Woodward, J., Russell, A. J., Fleisher, P. J., & Bailey, P. K. (2008). Controls on the sedimentary architecture of a single event englacial esker: Skeiðarárjökull, Iceland. *Quaternary Science Reviews*, *27*(19–20): 1829–1847. https://doi.org/10.1016/j.quascirev.2008.06.012

Burke, M. J., Woodward, J., Russell, A. J., Fleisher, P. J., & Bailey, P. K. (2010). The sedimentary architecture of outburst flood eskers: A comparison of ground-penetrating radar data from Bering Glacier, Alaska and Skeiarárjökull, Iceland. *Bulletin of the Geological Society of America*, *122*(9–10): 1637–1645. https://doi.org/10.1130/B30008.1

727   Burke, M.J., Brennand, T.A. and Perkins, A.J. (2012) Transient subglacial hydrology of a thin ice
728   sheet: insights from the Chasm esker, British Columbia, Canada. *Quaternary Science*
729   *Reviews*, *58*: 30-55.

730   Cassidy, N.J. and Jol, H.M. (2009) Ground penetrating radar data processing, modelling and
731   analysis. *Ground penetrating radar: theory and applications*: 141-176

732   Charlesworth, J.K. (1921). The glacial geology of the north-west of lreland. *Proceedings of the*
733   *Royal lrish Academy*, 36b: 174-314

734   Charlesworth, J.K. (1921) The Evishnoran "Esker", Tyrone. *Geological Magazine*, 63(5), 223-225.
735   doi:10.1017/S0016756800084156

736   Chiverrell, R.C., Thomas, G.S.P., Burke, M., Medialdea, A., Smedley, R., Bateman, M., Clark, C.,
737   Duller, G.A., Fabel, D., Jenkins, G. and Ou, X., 2020. The evolution of the terrestrial-
738   terminating Irish Sea glacier during the last glaciation. Journal of Quaternary Science

739   Clark, C.D. and Meehan, R.T. (2001) Subglacial bedform geomorphology of the Irish Ice Sheet
740   reveals major configuration changes during growth and decay. *Journal of Quaternary*
741   *Science: Published for the Quaternary Research Association*, *16*(5): 483-496

742   Clark, C.D., Ely, J.C., Greenwood, S.L., Hughes, A.L., Meehan, R., Barr, I.D., Bateman, M.D.,
743   Bradwell, T., Doole, J., Evans, D.J. and Jordan, C.J. (2018) BRITICE Glacial Map, version
744   2: a map and GIS database of glacial landforms of the last British–Irish Ice
745   Sheet. *Boreas*, *47*(1): 11

746   Clark, C.D., Hughes, A.L., Greenwood, S.L., Jordan, C. and Sejrup, H.P. (2012) Pattern and timing
747   of retreat of the last British-Irish Ice Sheet. *Quaternary Science Reviews*, *44*: 112-146

748   Clark, P. U., & Walder, J. S. (1994). Subglacial drainage, eskers, and deforming beds beneath the
749   Laurentide and Eurasian ice sheets. *Geological Society of America Bulletin*, *106*(2), 304–
750   314. https://doi.org/10.1130/0016-7606(1994)106<0304:SDEADB>2.3.CO;2

751   Cofaigh, C.Ó., Weilbach, K., Lloyd, J.M., Benetti, S., Callard, S.L., Purcell, C., Chiverrell, R.C.,
752   Dunlop, P., Saher, M., Livingstone, S.J. and Van Landeghem, K.J. (2019) Early deglaciation
753   of the British-Irish Ice Sheet on the Atlantic shelf northwest of Ireland driven by
754   glacioisostatic depression and high relative sea level. *Quaternary Science Reviews*, *208*: 76-
755   96.

756   Colhoun, A. (1971) The glacial stratigraphy of the Sperrin Mountains and its relation to the glacial
757   stratigraphy of north-west Ireland. Proceedings of the Royal Irish Academy 71B: 37–52

758   Colhoun, E.A. (1970). On the nature of the glaciations and final deglaciation of the Sperrin
759   Mountains and adjacent areas in the north of Ireland. *Irish Geography,* 6(2), 162-185.

760   Cummings, D.I., Kjarsgaard, B.A., Russell, H.A. and Sharpe, D.R. (2011) Eskers as mineral
761   exploration tools. *Earth-science reviews*, *109*(1-2): 32-43

762 Davison, B.J., Sole, A.J., Livingstone, S.J., Cowton, T.R. and Nienow, P.W. (2019) The influence of
763   hydrology on the dynamics of land-terminating sectors of the Greenland Ice Sheet. *Frontiers*
764   *in Earth Science*, 7.

765 Delaney, C. (2001a) Esker formation and the nature of deglaciation: the Ballymahon esker, Central
766   Ireland. *North West Geography*, *1*(2): 23-33

767 Delaney, C. (2001b) Morphology and sedimentology of the Rooskagh esker, Co. Roscommon. *Irish*
768   *Journal of Earth Sciences*: 5-22

769 Delaney, C. (2002) Sedimentology of a glaciofluvial landsystem, Lough Ree area, Central Ireland:
770   implications for ice margin characteristics during Devensian deglaciation. *Sedimentary*
771   *Geology*, *149*(1-3): 111-126

772 Delaney, C.A., McCarron, S. and Davis, S. (2018). Irish Ice Sheet dynamics during deglaciation of
773   the central Irish Midlands: Evidence of ice streaming and surging from airborne LiDAR.
774   *Geomorphology*, 306, 235-253.

775 Drews, R., Pattyn, F., Hewitt, I.J., Ng, F.S.L., Berger, S., Matsuoka, K., Helm, V., Bergeot, N.,
776   Favier, L. and Neckel, N. (2017) Actively evolving subglacial conduits and eskers initiate
777   ice shelf channels at an Antarctic grounding line. *Nature communications*, 8: 15228

778 Dyke, A. and Prest, V. (1987) Late Wisconsinan and Holocene history of the Laurentide ice
779   sheet. *Géographie physique et Quaternaire*, *41*(2): 237-263.

780 Evans, D. J. A., & Benn, D. I. (2004) A practical guide to the study of glacial sediments. Edward
781   Arnold, London.

782 Fiore, J., Pugin, A. and Beres, M. (2002) Sedimentological and GPR studies of subglacial deposits
783   in the Joux Valley (Vaud, Switzerland): backset accretion in an esker followed by an erosive
784   jökulhlaup. *Géographie physique et Quaternaire*, *56*(1): 19-32

785 Fitzsimons, S.J. (1991) Supraglacial eskers in Antarctica. *Geomorphology*, *4*(3-4): 293-299

786 Flint, R.F. (1930) The Origin of the Irish" Eskers". *Geographical Review*, *20*(4): 615-630

787 Franke, D., Hornung, J. and Hinderer, M. (2015) A combined study of radar facies, lithofacies and
788   three-dimensional architecture of an alpine alluvial fan (Illgraben fan,
789   Switzerland). *Sedimentology*, *62*(1): 57-86

790 Gawthorpe, R.L., Collier, R.L., Alexander, J., Bridge, J.S. and Leeder, M.R. (1993) Ground
791   penetrating radar: application to sandbody geometry and heterogeneity studies. *Geological*
792   *Society, London, Special Publications*, *73*(1): 421-432

793 Geological Survey Northern Ireland (2016) Digital Geological Map of Northern Ireland – 10k. 10k
794   geology reproduced with the permission of the Geological Survey of Northern Ireland.
795   Crown Copyright 2018.

796 Gorrell, G. and Shaw, J. (1991) Deposition in an esker, bead and fan complex, Lanark, Ontario,
797   Canada. *Sedimentary Geology*, *72*(3-4): 285-314

798 Greenwood, S.L., Clark, C.D. and Hughes, A.L., 2007. Formalising an inversion methodology for
799   reconstructing ice-sheet retreat patterns from meltwater channels: application to the British
800   Ice Sheet. *Journal of Quaternary Science: Published for the Quaternary Research*
801   *Association*, *22*(6), pp.637-645

802 Greenwood, S. L., & Clark, C. D. (2009a). Reconstructing the last Irish Ice Sheet 1: changing flow
803   geometries and ice flow dynamics deciphered from the glacial landform record. *Quaternary*
804   *Science Reviews*, *28*(27–28), 3085–3100. https://doi.org/10.1016/j.quascirev.2009.09.008

805 Greenwood, S. L., & Clark, C. D. (2009b). Reconstructing the last Irish Ice Sheet 2: a
806   geomorphologically-driven model of ice sheet growth, retreat and dynamics. *Quaternary*
807   *Science Reviews*, *28*(27–28), 3101–3123. https://doi.org/10.1016/j.quascirev.2009.09.014

808 Greenwood, S.L., Clason, C.C., Helanow, C. and Margold, M. (2016) Theoretical, contemporary
809   observational and palaeo-perspectives on ice sheet hydrology: processes and
810   products. *Earth-Science Reviews*, *155*: 1-27

811 Gregory, J.W. (1912) The relations of kames and eskers. *The Geographical Journal*, *40*(2): 169-175.

812 Gregory, J.W. (1921) IV.—The Irish eskers. *Phil. Trans. R. Soc. Lond. B*, *210*(372-381): 115-151.

813 Gregory, J.W. (1925) The Evishanoran Esker, 1 Tyrone. *Geological Magazine*, *62*(10): 451-458.

814 Gregory, J.W. (1926) The Evishnoran "Esker". *Geological Magazine*, 62(7): 336-336.

815   doi:10.1017/S0016756800084557

816 Gustavson, T.C. and Boothroyd, J.C. (1987) A depositional model for outwash, sediment sources,
817   and hydrologic characteristics, Malaspina Glacier, Alaska: A modern analog of the
818   southeastern margin of the Laurentide Ice Sheet. *Geological Society of America*
819   *Bulletin*, *99*(2): 187-200.

820 Hebrand, M. and Åmark, M. (1989) Esker formation and glacier dynamics in eastern Skane and
821   adjacent areas, southern Sweden. *Boreas*, *18*(1): 67-81.

822 Hewitt, I.J. and Creyts, T.T., 2019. A model for the formation of eskers. *Geophysical Research*
823   *Letters*, *46*(12), pp.6673-6680.

824 Hinch, J. (1921) The eskers of Ireland. *The Irish Naturalist*, *30*(12): 137-142

825 Hubbard, B. & Nienow, P. (1997) Alpine subglacial hydrology. *Quaternary Science Reviews*, 16,
826   939-955.

827 Iken, A., Bindschadler, R.A. (1986). Combined measurements of subglacial water pressure and
828   surface velocity of Findelengletscher, Switzerland: conclusions about drainage system and
829   sliding mechanism. Journal of Glaciology, 32(110), 101-119.

830 Jol, H.M. and Smith, D.G. (1991) Ground penetrating radar of northern lacustrine deltas. *Canadian*
831   *Journal of Earth Sciences*, *28*(12): 1939-1947

832   Knight, J. (1997). Morphological and morphometric analysis of drumlin bedforms in the Omagh
833   Basin, north central Ireland. *Geografiska Annaler,* 79A: 255-266.

834   Knight, J. (1999). Geological evidence for neotectonic activity during deglaciation of the southern
835   Sperrin Mountains, Northern Ireland. *Journal of Quaternary Science,* 14(1), 45-57.

836   Knight, J. (2003). Bedform patterns, subglacial meltwater events, and Late Devensian ice sheet
837   dynamics in north-central Ireland. *Global and Planetary Change*, 35(3–4), 237–253.

838   Knight, J. (2006) Geomorphic evidence for active and inactive phases of Late Devensian ice in
839   north-central Ireland. *Geomorphology*, 75(1-2): 4-19

840   Knight, J. (2019) The geomorphology and sedimentology of eskers in north-Central
841   Ireland. *Sedimentary Geology*, 382: 1-24.

842   Knight, J. and McCabe, A.M. (1997) Identification and significance of ice-flow-transverse
843   subglacial ridges (Rogen moraines) in northern central Ireland. *Journal of Quaternary
844   Science*, 12(6): 519-524

845   Knight, J., Coxon, P., McCabe, A.M. and McCarron, S.G. (2004) Pleistocene glaciations in Ireland.
846   In *Developments in Quaternary Sciences* (Vol. 2, pp. 183-191). Elsevier

847   Knight, J., Coxon, P., McCabe, A.M. and McCarron, S.G. (2004) Pleistocene glaciations in Ireland.
848   In *Developments in Quaternary Sciences* (Vol. 2, pp. 183-191). Elsevier.

849   Livingstone, S. J., Utting, D. J., Ruffell, A., Clark, C. D., Pawley, S., Atkinson, N., & Fowler, A. C.
850   (2016). Discovery of relict subglacial lakes and their geometry and mechanism of drainage.
851   *Nature Communications*, 7. https://doi.org/10.1038/ncomms11767

852   Livingstone, S.J., Storrar, R.D., Hillier, J.K., Stokes, C.R., Clark, C.D. and Tarasov, L. (2015) An
853   ice-sheet scale comparison of eskers with modelled subglacial drainage
854   routes. *Geomorphology*, 246: 104-112

855   Livingstone, S.J., Lewington, E.L., Clark, C.D., Storrar, R.D., Sole, A.J., McMartin, I., Dewald, N.
856   and Ng, F., 2020. A quasi-annual record of time-transgressive esker formation: implications
857   for ice-sheet reconstruction and subglacial hydrology. *The Cryosphere*, 14(6), pp.1989-2004

858   Mäkinen, J. (2003) Time-transgressive deposits of repeated depositional sequences within
859   interlobate glaciofluvial (esker) sediments in Köyliö, SW Finland. *Sedimentology*, 50(2):
860   327-360

861   Margold, M., Jansson, K.N., Kleman, J., Stroeven, A.P. and Clague, J.J. (2013) Retreat pattern of
862   the Cordilleran Ice Sheet in central British Columbia at the end of the last glaciation
863   reconstructed from glacial meltwater landforms. *Boreas*, 42(4): 830-847

864   McCabe, A.M. (2008) *Glacial geology and geomorphology: the landscapes of Ireland*. Dunedin
865   Academic Press Ltd.

866   McCarron, S., 2014. Deglaciation of the Dungiven Basin, North-West Ireland. *Irish Journal of Earth
867   Sciences*, 31, pp.43-71

868 Miall, A.D. (1985) Architectural-element analysis: a new method of facies analysis applied to fluvial
869   deposits. *Earth Sci. Rev.*, 22, 261–308

870 Neal, A. (2004) Ground-penetrating radar and its use in sedimentology: principles, problems and
871   progress. *Earth-science reviews*, *66*(3-4): 261-330

872 Ó Cofaigh, C., Evans, D.J.A. (2007) Radiocarbon constraints on the age of the maximum advance of
873   the British-Irish Ice Sheet in the Celtic Sea. Quaternary Science Reviews 26 (9–10), 1197–
874   1203

875 Pellicer, X. M., & Gibson, P. (2011). Electrical resistivity and Ground Penetrating Radar for the
876   characterisation of the internal architecture of Quaternary sediments in the Midlands of
877   Ireland. *Journal of Applied Geophysics*, *75*(4), 638–647.
878   https://doi.org/10.1016/j.jappgeo.2011.09.019

879 Pellicer, X. M., Warren, W. P., Gibson, P., & Linares, R. (2012). Construction of an evolutionary
880   deglaciation model for the Irish midlands based on the integration of morphostratigraphic
881   and geophysical data analyses. *Journal of Quaternary Science*, *27*(8), 807–818.
882   https://doi.org/10.1002/jqs.2570

883 Perkins, A. J., Brennand, T. A., & Burke, M. J. (2016). Towards a morphogenetic classification of
884   eskers: Implications for modelling ice sheet hydrology. *Quaternary Science Reviews*, *134*,
885   19–38. https://doi.org/10.1016/j.quascirev.2015.12.015

886 Perkins, A.J., Brennand, T.A. and Burke, M.J. (2013) Genesis of an esker-like ridge over the
887   southern Fraser Plateau, British Columbia: Implications for paleo-ice sheet reconstruction
888   based on geomorphic inversion. *Geomorphology*, *190*:27-39

889 Price, R.J. (1969) Moraines, sandar, kames and eskers near Breidamerkurjökull,
890   Iceland. *Transactions of the Institute of British Geographers*: 17-43

891 Roberts, M.C., Niller, H.P. and Helmstetter, N. (2003) Sedimentary architecture and radar facies of a
892   fan delta, Cypress Creek, West Vancouver, British Columbia. *Geological Society, London,*
893   *Special Publications*, *211*(1): 111-126

894 Röthlisberger, H. (1972) Water pressure in intra-and subglacial channels. *Journal of*
895   *Glaciology*, *11*(62): 177-203

896 Russell, A.J., Knudsen, O., Fay, H., Marren, P.M., Heinz, J. and Tronicke, J. (2001) Morphology
897   and sedimentology of a giant supraglacial, ice-walled, jökulhlaup channel, Skeiðarárjökull,
898   Iceland: implications for esker genesis. *Global and Planetary Change*, *28*(1-4): 193-216

899 Rust, B.R. (1977) Mass flow deposits in a Quaternary succession near Ottawa, Canada: diagnostic
900   criteria for subaqueous outwash. *Canadian Journal of Earth Science*, 14: 175-184

901 Sambrook-Smith, G.H., Ashworth, P.J., Best, J.L., Woodward, J. and Simpson, C.J. (2006) The
902   sedimentology and alluvial architecture of the sandy braided South Saskatchewan River,
903   Canada. *Sedimentology*, *53*(2): 413-434

904   Saunderson, H.C. (1977) The sliding bed facies in esker sands and gravels: a criterion for full-pipe
905   (tunnel) flow? *Sedimentology*, *24*(5):623-638

906   Schoof, C. (2010) Ice-sheet acceleration driven by melt supply variability. *Nature*, *468*(7325): 803

907   Shreve, R. L. (1985). Esker characteristics in terms of glacier physics, Katahdin esker system,
908   Maine. *Geological Society of America Bulletin*, *96*(5), 639–646.
909   https://doi.org/10.1130/0016-7606(1985)96<639:ECITOG>2.0.CO;2

910   Smith, M. J. & Clark, C. D. (2005) Methods for the visualization of digital elevation models for
911   landform mapping. *Earth Surface Processes and Landforms*, 30, 885-900

912   Smith, M.J. and Clark, C.D. (2005) Methods for the visualization of digital elevation models for
913   landform mapping. *Earth Surface Processes and Landforms*, *30*(7): 885-900

914   Smith, M.J. and Knight, J. (2011) Palaeoglaciology of the last Irish Ice Sheet reconstructed from
915   striae evidence. *Quaternary Science Reviews,* 30(1-2): 147-160

916   Sollas, W.J. (1896) A map to show the Distribution of Eskers in Ireland. *Sci. Trans. R. Dublin Soc,*
917   2(5): 785-822.

918   Stearns, L.A., Smith, B.E. and Hamilton, G.S. (2008). Increased flow speed on a large East
919   Antarctic outlet glacier caused by subglacial floods. Nature Geoscience, 1(12), 827-831.

920   Storrar, R.D., Ewertowski, M., Tomczyk, A.M., Barr, I.D., Livingstone, S.J., Ruffell, A., Stoker,
921   B.J. and Evans, D.J. (2020) Equifinality and preservation potential of complex
922   eskers. *Boreas*, 49(1), 211-231.

923   Storrar, R. D., Evans, D. J. A., Stokes, C. R., & Ewertowski, M. (2015). Controls on the location,
924   morphology and evolution of complex esker systems at decadal timescales,
925   Breidamerkurjökull, southeast Iceland. *Earth Surface Processes and Landforms*, *40*(11),
926   1421–1438. https://doi.org/10.1002/esp.3725

927   Storrar, R.D., Stokes, C.R. and Evans, D.J. (2013) A map of large Canadian eskers from Landsat
928   satellite imagery. *Journal of maps*, *9*(3): 456-473

929   Storrar, R.D., Stokes, C.R. and Evans, D.J. (2014a) Morphometry and pattern of a large sample (>
930   20,000) of Canadian eskers and implications for subglacial drainage beneath ice
931   sheets. *Quaternary Science Reviews*, *105*: 1-25

932   Storrar, R.D., Stokes, C.R. and Evans, D.J. (2014b) Increased channelization of subglacial drainage
933   during deglaciation of the Laurentide Ice Sheet. *Geology*, *42*(3): 239-242

934   Stroeven, A. P., Hättestrand, C., Kleman, J., Heyman, J., Fabel, D., Fredin, O., Goodfellow, B. W.,
935   Harbor, J. M., Jansen, J. D., Olsen, L., Caffee, M. W., Fink, D., Lundqvist, J., Rosqvist, G.
936   C., Strömberg, B. & Jansson, K. N. (2016) Deglaciation of Fennoscandia. *Quaternary*
937   *Science Reviews*, 147, 91-121.

938   Warren, W.P. and Ashley, G.M. (1994) Origins of the ice-contact stratified ridges (eskers) of
939   Ireland. *Journal of Sedimentary Research*, *64*(3a): 433-449

940   Wilson, P., Ballantyne, C.K., Benetti, S., Small, D., Fabel, D. and Clark, C.D., 2019. Deglaciation
941   chronology of the Donegal Ice Centre, north-west Ireland. Journal of Quaternary Science,
942   34(1), pp.16-28

943

944   Winsemann, J., Asprion, U., Meyer, T. and Schramm, C. (2007) Facies characteristics of Middle
945   Pleistocene (Saalian) ice-margin subaqueous fan and delta deposits, glacial Lake Leine, NW
946   Germany. *Sedimentary Geology*, *193*(1-4): 105-129

947   Wright, A. P., Siegert, M. J., Le Brocq, A. M., & Gore, D. B. (2008). High sensitivity of subglacial
948   hydrological pathways in Antarctica to small ice-sheet changes. *Geophysical Research*
949   *Letters*, *35*(17), 1–5. https://doi.org/10.1029/2008GL034937

950   Zwally, H.J., et al. (2002). Surface melt-induced acceleration of Greenland ice-sheet flow. Science,
951   297(5579), 218-222.

952

953

954